

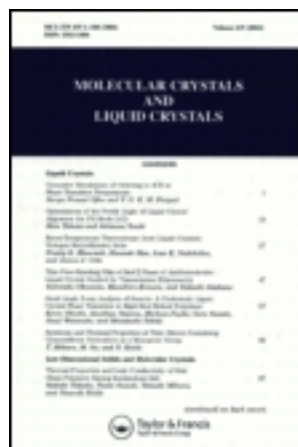
This article was downloaded by: [Tomsk State University of Control Systems and Radio]

On: 19 February 2013, At: 12:44

Publisher: Taylor & Francis

Informa Ltd Registered in England and Wales Registered Number: 1072954

Registered office: Mortimer House, 37-41 Mortimer Street, London W1T 3JH, UK



Molecular Crystals and Liquid Crystals Incorporating Nonlinear Optics

Publication details, including instructions for authors and subscription information:

<http://www.tandfonline.com/loi/gmcl17>

Thermodynamic Model of Ferroelectric Chiral Smectic C* Liquid Crystals

T. Carlsson^a, B. žekš^{b c}, C. Filipič^b, A. Levstik^b & R. Blinc^b

^a Institute of Theoretical Physics, Chalmers University of Technology, S-412 96, Göteborg, Sweden

^b J. Stefan Institute, University of Ljubljana, Jamova 39, YU-61111, Ljubljana, Yugoslavia

^c Institute of Biophysics, Medical Faculty, University of Ljubljana, Lipičeva 2, YU-61105, Ljubljana, Yugoslavia

Version of record first published: 03 Jan 2007.

To cite this article: T. Carlsson, B. žekš, C. Filipič, A. Levstik & R. Blinc (1988): Thermodynamic Model of Ferroelectric Chiral Smectic C* Liquid Crystals, *Molecular Crystals and Liquid Crystals Incorporating Nonlinear Optics*, 163:1, 11-72

To link to this article: <http://dx.doi.org/10.1080/00268948808081988>

PLEASE SCROLL DOWN FOR ARTICLE

Full terms and conditions of use: <http://www.tandfonline.com/page/terms-and-conditions>

This article may be used for research, teaching, and private study purposes. Any substantial or systematic reproduction, redistribution, reselling, loan, sub-licensing, systematic supply, or distribution in any form to anyone is expressly forbidden.

The publisher does not give any warranty express or implied or make any representation that the contents will be complete or accurate or up to date. The accuracy of any instructions, formulae, and drug doses should be independently verified with primary sources. The publisher shall not be liable for any loss, actions, claims, proceedings, demand, or costs or damages whatsoever or howsoever caused arising directly or indirectly in connection with or arising out of the use of this material.

Mol. Cryst. Liq. Cryst., 1988, Vol. 163, pp. 11–72
Reprints available directly from the publisher
Photocopying permitted by license only
© 1988 Gordon and Breach Science Publishers S.A.
Printed in the United States of America

Thermodynamic Model of Ferroelectric Chiral Smectic C* Liquid Crystals

T. CARLSSON

*Institute of Theoretical Physics, Chalmers University of Technology, S-412 96
Göteborg, Sweden*

and

B. ŽEKŠ,† C. FILIPIČ, A. LEVSTIK and R. BLINC

*J. Stefan Institute, University of Ljubljana, Jamova 39, YU-61111 Ljubljana,
Yugoslavia*

(Received February 6, 1987; in final form September 30, 1987)

A thermodynamic model of the ferroelectric SmC* phase, based on an extended Landau expansion of the free-energy density, is presented. We discuss how the signs of the parameters entering the model are depending on whether the pitch of the helix is right-handed or left-handed and whether the compound is of the (+) or (−) type in regard to the sign of the polarization. With the introduced Landau expansion as a basis, we derive the equations governing the behaviour of the tilt, polarization, pitch, dielectric susceptibility and heat capacity of the system. We show that by rewriting the equations into dimensionless form, we can transform the original set of eleven parameters in the Landau expansion into a new set, consisting of six dimensionless parameters and five scaling factors. The six dimensionless parameters are the only ones which enter the calculations of the quantities mentioned above, i.e. we need six dimensionless parameters to describe the temperature dependence of the five basic quantities of the system.

By solving the governing equations we investigate the influence of the parameters on the behaviour of the system. We show that, concerning the calculation of tilt and polarization, only three parameters have to be taken into account under reasonable assumptions. Furthermore we show, that the behaviour of the ratio polarization/tilt versus tilt-squared is determined by one parameter only. It is also shown that our model predicts, for large enough tilt, a sign reversal of the polarization. Finally a

†Institute of Biophysics, Medical Faculty, University of Ljubljana, Lipičeva 2, YU-61105 Ljubljana, Yugoslavia

simple relation is derived, connecting the Goldstone mode part of the dielectric susceptibility to the quantities polarization, tilt and pitch. This relation is verified as well by numerical calculations as by comparison to experimental data.

Keywords: Chiral smectic, ferroelectric, phase transition, Landau expansion, polarization, susceptibility

TABLE OF CONTENTS

I.	Introduction	12
II.	Equations governing the behaviour of ferroelectric, SmC* liquid crystals.....	14
II.1	Landau expansion of the free-energy density	14
II.2	Equations governing the tilt, polarization and pitch	18
II.3	Derivation of the SmA–SmC* phase transition temperature.....	19
II.4	Dimensionless form of the equations	20
II.5	Symmetry properties of the governing equations—possible temperature dependences of the pitch....	23
II.6	Unwinding of the helix	28
II.7	The static dielectric susceptibility	32
II.8	The heat capacity	42
III.	General behaviour of the solutions of the governing equations—comparison with experimental data	43
III.1	An estimation of the material parameters of DO-BAMBC—general features of the parameters.....	43
III.2	A quantitative estimation of the magnitude of the effects due to the unwinding of the helix.....	47
III.3	Analytical solution of the polarization equation—the possibility of sign reversal of the polarization	48
III.4	General behaviour of the solutions of the equations governing tilt and polarization.....	51
III.5	Behaviour of the pitch	58
III.6	The static dielectric susceptibility	60
III.7	The heat capacity	67
IV.	Discussion.....	68

I. INTRODUCTION

Chiral SmC* liquid crystals exhibit ferroelectric behaviour¹ and have gained an increasing amount of interest during the last years. Grad-

usually, a lot of experimental information has become available and today at least the qualitative behaviour of many important quantities can be considered to be established in the literature. In this context we refer to the temperature dependence of tilt,^{2,3} spontaneous polarization,^{2,4-9} pitch,^{2,10,11} dielectric susceptibility^{2,4,12-18} and heat capacity¹⁹⁻²¹ of the system. The SmC* liquid crystals are layered structures, where the molecules within each layer are tilted with respect to the normal to the smectic layers. The tilt of the long molecular axis precesses as one goes from one smectic layer to another, resulting in a helicoidal structure. Because of the chirality of molecules the tilt locally breaks the axial symmetry around the molecular axis and induces a transverse inplane polarization perpendicular to the direction of the tilt.¹ Early attempts^{22,23} of constructing a theoretical model of the ferroelectric SmC* phase based on a Landau expansion of the free-energy density have failed to describe the temperature dependence of the basic quantities of the system in a proper way. The most serious disagreements between the prediction of the theory and existing experimental data are the following:

- i) The model predicts the polarization P_o to be proportional to the tilt θ_o , i.e. $P_o/\theta_o = \text{constant}$, in all the SmC* phase. This is not in accordance with the observed experimental behaviour,^{2,6,7} showing that the ratio P_o/θ_o is a temperature dependent quantity.
- ii) The measured polarization for DOBAMBC⁶ and also for other compounds^{8,9} displays an S-shaped temperature dependence in the SmC* phase approximately 1K below the SmA-SmC* phase transition temperature T_c . This is in contrast to the classical square-root dependence predicted by the model.
- iii) The pitch of the helix which should be temperature independent according to the model, slowly increases with increasing temperature, reaches a maximum at approximately 1K below T_c and then sharply decreases to a finite value at T_c .^{2,10,11}
- iv) The dielectric constant is predicted by the model to exhibit a cusp-like maximum at T_c . In experiments however, a broad continuous maximum shows up a few degrees below T_c .^{12-14,17,18}

In this work we show that by using a generalized Landau expansion, where the most essential thing is the introduction of a biquadratic coupling between tilt and polarization,^{6,24} we are able to describe the behaviour of most of the quantities of interest for a ferroelectric SmC* liquid crystal. By comparing the calculations with experimental data we show that our theory is not only capable to reproduce the qualitative behaviour of the system but also, concerning most data, the

quantitative behaviour in a decent way. We are also able to show that not only the anomalous behaviour of the pitch^{2,10,11} but also the anomalous behaviour of polarization (i.e. different square-root temperature dependence close to and far from the transition to the SmA phase) which has been observed by some authors^{6,8,9} is a natural consequence of the theory and can also be expected, in a less pronounced way, to be exhibited by the tilt. The outline of the paper is as follows:

In Section II we introduce an extended Landau type expansion of the free-energy density of SmC* liquid crystals. With this as a starting point we then derive the equations governing the behaviour of quantities such as the tilt, polarization, pitch, dielectric susceptibility and heat capacity of the system. We also show that by rewriting all the equations into dimensionless form we can reduce the number of independent parameters introduced by the Landau expansion to six—i.e. we show that we need six dimensionless parameters to describe the temperature dependence of five experimentally determined quantities.

In Section III we solve the governing equations of the system analytically as far as possible and numerically, comparing the results with available experimental data. By doing so we show, that all the shortcomings of the simpler model which were mentioned above (points (i)–(iv)) have been removed and that our model gives a theoretical picture of the SmC* phase which is in good agreement with the experimental behaviour of the system. We also discuss the influence of the parameters of the model on the behaviour of the solution of the governing equations.

II. EQUATIONS GOVERNING THE BEHAVIOUR OF FERROELECTRIC, SmC* LIQUID CRYSTALS

II.1 Landau expansion of the free-energy density

The purpose of this work is to develop a theory which can properly describe the temperature dependence of quantities such as the tilt (θ_o), the polarization (P_o), the pitch (p), the dielectric response (χ) and the heat capacity (C_p) of a ferroelectric SmC* liquid crystal. We will base our model on a Landau type expansion where the free-energy density of the system is expanded in two order parameters. These are the primary order parameter, the two component tilt vector ξ , which is the projection of the director \hat{n} into the smectic planes, and the two component in-plane polarization \mathbf{P} which is always¹ at right angle to ξ . The coordinates we use are defined in Figure 1. The

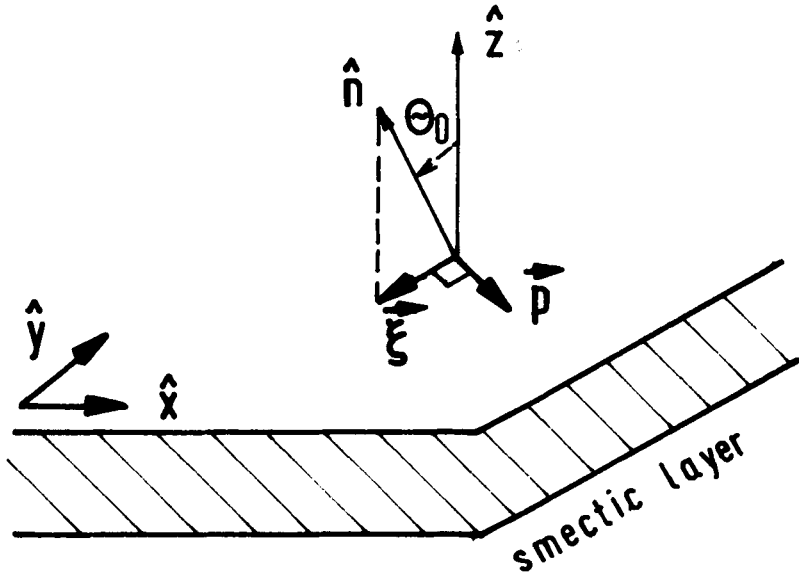


FIGURE 1 Definition of coordinates and introduction of the order parameters ξ and \mathbf{P} .

smectic planes are assumed to be parallel to the xy plane and the modulation of the system is along the z axis, while \hat{n} and \hat{z} are chosen with their signs in such a way that $\hat{n} \cdot \hat{z} > 0$. The order parameters can thus be written $\xi = \xi_1 \hat{x} + \xi_2 \hat{y}$ and $\mathbf{P} = P_x \hat{x} + P_y \hat{y}$, respectively.

The free-energy density which we will use was first introduced by Žekš,²⁴ except for the sixth order term in the tilt which was independently introduced by Huang and Viner¹⁹ and by Carlsson and Dahl.²⁰

$$\begin{aligned}
 g_o(z) = & \frac{1}{2}a(\xi_1^2 + \xi_2^2) + \frac{1}{4}b(\xi_1^2 + \xi_2^2)^2 + \frac{1}{6}c(\xi_1^2 + \xi_2^2)^3 \\
 & - \Lambda \left(\xi_1 \frac{d\xi_2}{dz} - \xi_2 \frac{d\xi_1}{dz} \right) + \frac{1}{2}K_3 \left[\left(\frac{d\xi_1}{dz} \right)^2 + \left(\frac{d\xi_2}{dz} \right)^2 \right] \\
 & - d(\xi_1^2 + \xi_2^2) \left(\xi_1 \frac{d\xi_2}{dz} - \xi_2 \frac{d\xi_1}{dz} \right) + \frac{1}{2\epsilon} (P_x^2 + P_y^2) \quad (II.1) \\
 & + \frac{1}{4}\eta(P_x^2 + P_y^2)^2 - \mu \left(P_x \frac{d\xi_1}{dz} + P_y \frac{d\xi_2}{dz} \right) \\
 & + C(P_x \xi_2 - P_y \xi_1) - \frac{1}{2}\Omega(P_x \xi_2 - P_y \xi_1)^2
 \end{aligned}$$

The only of the coefficients introduced in Eq. (II.1), which is assumed to be temperature dependent is $a = \alpha(T - T_o)$, T being the temperature of the system. The constant T_o corresponds to the phase transition temperature of the corresponding racemic mixture (i.e. with the chiral coefficients Λ , C and d put equal to zero). The first two terms in Eq. (II.1) are the usual quadratic and fourth-order terms included in the Landau expansion of the free-energy density of a system being close to a second-order phase transition. If the free-energy density shall be capable of describing the heat capacity of the system in a correct way,^{19,20} we also have to add a sixth-order term in tilt and for this purpose we introduce the constant c . The elastic modulus is denoted by K_3 , the coefficient of the Lifshitz term responsible for the modulation is denoted by Λ and μ and C are the coefficients of the flexo- and piezo-electric bilinear coupling. The dielectric constant of the system in the high temperature limit of the SmA phase is denoted ϵ while Ω is the coefficient of the biquadratic coupling term inducing transverse quadrupole ordering and the η -term has been added to stabilize the system. The d -term is describing the monotonous increase of the pitch with temperature at low temperature. While we can assume, by physical reasons, the constants α , b , c , K_3 , ϵ and η to be positive, the signs of Λ , μ , C and d can be allowed to adopt both positive or negative values. The signs of the four last constants will depend on whether the helix of the pitch is right-handed (RH) or left-handed (LH) and whether the compound is a (+) or a (−) substance according to the nomenclature of Clark and Lagerwall.²⁵ (The exact definition of the meaning of (+) and (−) substances is given below). In Section II.5 we will derive the connections between the signs of Λ , μ , C and d and the type (RH(+), RH(−), LH(+)) or LH(−)) to which a certain compound belongs. Furthermore we only treat the case when Ω is positive.

The above model does not represent a systematic expansion of the free energy as a function of the two order parameters ξ and \mathbf{P} and only those higher order terms are included, which correspond to a particular physical mechanism and which essentially influence the behaviour of the system. The most relevant new term is the biquadratic coupling term between tilt and polarization (the Ω -term). This term, which has been first introduced by Žekš,²⁴ describes the fact that the tilt induces a transverse quadrupole moment in chiral as well as non-chiral SmC systems. Such quadrupole moments were experimentally observed by NMR^{26–29} in SmC* and SmC liquid crystals and they were shown to be proportional to the square of the tilt. They are large compared to induced dipole moments in SmC* phase

(not very close to T_c) and point in the same direction as dipole moments, i.e. perpendicular to the direction of the tilt. This corresponds in our notation to $\Omega > 0$ and therefore only this case will be treated here. As the biquadratic coupling is quadratic in tilt in contrast to the bilinear coupling the cross-over behaviour is introduced into the model in SmC^* phase from the bilinear coupling regime close to T_c to the regime at lower temperature, where the biquadratic coupling becomes relevant. This cross-over causes an almost nonanalytic behaviour and therefore qualitatively changes the properties of the system. Other higher order terms, which were not included into the model (Eq. II.1), would only quantitatively influence the system, i.e. their effect would be important if they were large.

The sixth order term in the tilt (the c -term) has been first introduced independently by two groups^{19,20} as a consequence of the observation that in ferroelectric liquid crystalline systems (e.g. DOBAMBC) SmA-SmC^* phase transition is of second order but close to a tricritical point. The c -term has been first added to the generalized Landau model by C. C. Huang and S. Dumrongrattana³⁰ and it was shown^{6,7,17,18,30,31} that the model can account for observed anomalous properties of DOBAMBC. It is believed that the model could represent a good description of ferroelectric liquid crystals in general and therefore here a systematic analysis of various thermodynamic properties of the model will be presented and the effect of model parameters will be studied.

In order to get any useful information out of Eq. (II.1) we have to make some reasonable assumptions concerning the order parameters ξ and \mathbf{P} . As we are studying the system close to the transition to the SmA phase, we know that the tilt is small. Thus we can make the approximation $|\xi| = \sin\theta_o \approx \theta_o$. As pointed out before the polarization is always mutually perpendicular to both ξ and \hat{z} . For given ξ and \hat{z} there are therefore two possible directions of \mathbf{P} . If ξ , \mathbf{P} and \hat{z} form a right-handed coordinate system, the compound is a (+) substance. If, on the other hand, ξ , \mathbf{P} and \hat{z} form a left-handed system we have a (−) substance. Introducing the wave vector of the pitch $q = 2\pi/p$ and letting a positive P_o correspond a (+) substance we make the following ansatz of the order parameters:

$$\begin{aligned} \xi_1 &= \theta_o \cos qz, & \xi_2 &= \theta_o \sin qz \\ P_x &= -P_o \sin qz, & P_y &= P_o \cos qz \end{aligned} \quad (\text{II.2})$$

Substituting Eqs. (II.2) into Eq. (II.1) we get the expression for the

free-energy density of the system which we will use as a starting-point for our further investigations

$$g_o(z) = \frac{1}{2}a\theta_o^2 + \frac{1}{4}b\theta_o^4 + \frac{1}{6}c\theta_o^6 - \Lambda q\theta_o^2 + \frac{1}{2}K_3q^2\theta_o^2 + \frac{1}{2\epsilon}P_o^2 \\ - \mu qP_o\theta_o - CP_o\theta_o - \frac{1}{2}\Omega P_o^2\theta_o^2 + \frac{1}{4}\eta P_o^4 - dq\theta_o^4 \quad (\text{II.3})$$

As a final remark we point out that if we, in the ansatz (II.2), had introduced \mathbf{P} at an arbitrary angle to ξ (i.e. by writing $P_x = -P_o \sin(qz + \varphi_o)$, $P_y = P_o \cos(qz + \varphi_o)$), we had arrived at an expression of the free energy density which adopted its minimum (in the case $\Omega > 0$) for $\sin\varphi_o = 0$. This means that the condition $\xi \cdot \mathbf{P} = 0$ comes out as a natural consequence of our model.

II.2 Equations governing tilt, polarization and pitch

We now are in a position to derive the equations governing the tilt, polarization and pitch of an undisturbed SmC* liquid crystal. The free-energy density is given by Eq. (II.3). Minimizing this with respect to q gives

$$q = \frac{\Lambda}{K_3} + \frac{\mu P_o}{K_3\theta_o} + \frac{d\theta_o^2}{K_3} \quad (\text{II.4})$$

We thus have obtained an expression of the pitch $p = 2\pi/q$ as a function of the tilt and the polarization.

To derive the equation which we will denote the tilt equation we minimize Eq. (II.3) with respect to θ_o and get

$$a\theta_o + b\theta_o^3 + c\theta_o^5 - 2\Lambda q\theta_o + K_3q^2\theta_o - \mu qP_o \\ - CP_o - \Omega P_o^2\theta_o - 4dq\theta_o^3 = 0 \quad (\text{II.5})$$

By substituting Eq. (II.4) into Eq. (II.5) we eliminate q from the tilt equation

$$\left(a - \frac{\Lambda^2}{K_3}\right)\theta_o + \left(b - \frac{4\Lambda d}{K_3}\right)\theta_o^3 + \left(c - \frac{3d^2}{K_3}\right)\theta_o^5 \\ - \Omega\theta_o P_o^2 - \left(C + \frac{\Lambda\mu}{K_3}\right)P_o - \frac{3d\mu}{K_3}\theta_o^2 P_o = 0 \quad (\text{II.6})$$

Minimizing Eq. (II.3) with respect to P_o gives the equation which we will denote the polarization equation

$$\frac{1}{\epsilon} P_o - \mu q \theta_o - C \theta_o - \Omega P_o \theta_o^2 + \eta P_o^3 = 0 \quad (\text{II.7})$$

By substituting Eq. (II.4) into Eq. (II.7) we eliminate q from the polarization equation

$$\left(\frac{1}{\epsilon} - \frac{\mu^2}{K_3} \right) P_o - \left(C + \frac{\Lambda \mu}{K_3} \right) \theta_o - \Omega P_o \theta_o^2 + \eta P_o^3 - \frac{\mu d}{K_3} \theta_o^3 = 0 \quad (\text{II.8})$$

We thus have obtained a pair of coupled equations (Eqs. (II.6) and (II.8)) which now have to be solved numerically. This is most easily done by the following procedure. Starting with a value of θ_o as an input parameter, Eq. (II.8) provides a cubic equation determining P_o . Substituting θ_o and P_o into Eq. (II.4) now gives q . Substituting θ_o and P_o into Eq. (II.6) admits us directly to calculate $a = \alpha(T - T_o)$ giving the corresponding temperature. By varying the input parameter θ_o over an appropriate interval we thus have calculated $\theta_o(T)$, $P_o(T)$ and $p(T)$.

II.3 Derivation of the SmA – SmC* phase transition temperature

In this section we will derive the expression of the phase transition temperature, T_c , which our model gives. At the phase transition both θ_o and P_o go towards zero in such a way that the ratio P_o/θ_o stays finite. In this limit Eq. (II.6) can be written as

$$\alpha(T_c - T_o) - \frac{\Lambda^2}{K_3} - \left(C + \frac{\Lambda \mu}{K_3} \right) \frac{P_o}{\theta_o} \Big|_{T \rightarrow T_c} = 0 \quad (\text{II.9})$$

Dividing Eq. (II.8) by θ_o and taking the limit $T \rightarrow T_c$ we get

$$\left(\frac{1}{\epsilon} - \frac{\mu^2}{K_3} \right) \frac{P_o}{\theta_o} \Big|_{T \rightarrow T_c} - \left(C + \frac{\Lambda \mu}{K_3} \right) = 0 \quad (\text{II.10})$$

which directly gives the ratio P_o/θ_o at the phase transition.

$$\lim_{T \rightarrow T_c} \frac{P_o}{\theta_o} = \left(C + \frac{\Lambda \mu}{K_3} \right) / \left(\frac{1}{\epsilon} - \frac{\mu^2}{K_3} \right) \quad (\text{II.11})$$

Substituting Eq. (II.11) into Eq. (II.9), the latter can be rearranged to read

$$T_c = T_o + \frac{1}{\alpha} \left[\frac{\Lambda^2}{K_3} + \left(C + \frac{\Lambda\mu}{K_3} \right)^2 / \left(\frac{1}{\epsilon} - \frac{\mu^2}{K_3} \right) \right] \quad (\text{II.12})$$

We thus see that the phase transition temperature has been slightly shifted for the SmC* liquid crystal in comparison with its racemic mixture.

II.4 Dimensionless form of the equations

In order to be able to describe correctly the temperature dependence of the quantities we want to study, we had to write down a Landau expansion of the free-energy density in which eleven parameters are introduced (Eq. (II.1)). This vast number of parameters will of course create problems for the experimentalist who is asked to determine them as well as for the theorist who is set to investigate how the variation of the different parameters affects the behaviour of the system. In this section we will show however, how we by renormalizing some of the constants and also by rewriting the equations into dimensionless form, can reduce the number of free parameters. In order to describe the temperature dependence of the five experimentally observable quantities of which we have interest, we will need only six independent parameters. In the end we also need to introduce five scaling factors, one for each physical quantity, which will enable us to compare the calculated, dimensionless quantities with the experimentally measured ones.

By inspection of Eqs. (II.6) and (II.8) we find a natural way of renormalizing the constants a , b , c , ϵ and C . Letting a tilde over the appropriate constant denote its renormalized form we get

$$\begin{aligned} \tilde{a} &= a - \frac{\Lambda^2}{K_3}, & \tilde{b} &= b - \frac{4\Lambda d}{K_3} \\ \tilde{c} &= c - \frac{3d^2}{K_3}, & \frac{1}{\tilde{\epsilon}} &= \frac{1}{\epsilon} - \frac{\mu^2}{K_3} \\ \tilde{C} &= C + \frac{\Lambda\mu}{K_3} \end{aligned} \quad (\text{II.13})$$

Introducing Eqs. (II.13) into the expression of the free-energy density (Eq. (II.3)) as well as substituting into it the expression of q given by Eq. (II.4) we get

$$g_o(z) = \frac{1}{2}\tilde{a}\theta_o^2 + \frac{1}{4}\tilde{b}\theta_o^4 + \frac{1}{6}\tilde{c}\theta_o^6 + \frac{1}{2\tilde{\epsilon}}P_o^2 - \tilde{C}P_o\theta_o - \frac{1}{2}\Omega P_o^2\theta_o^2 + \frac{1}{4}\eta P_o^4 - \frac{\mu d}{K_3}P_o\theta_o^3 \quad (\text{II.14})$$

It is an easy task to check that this way of writing the free-energy density enables us to derive the tilt equation (II.6) and the polarization equation (II.8) by minimizing $g_o(z)$ with respect to θ_o and P_o respectively.

The next step is to rewrite the equations into dimensionless form. To do so we first introduce six dimensionless constants according to

$$\gamma = \frac{\tilde{b}\eta}{\Omega^2}, \quad \beta = \frac{\eta^{1/2}\tilde{C}\tilde{\epsilon}}{\Omega^{1/2}}, \quad \rho = \frac{\tilde{c}\eta}{\tilde{\epsilon}\Omega^3}$$

$$\lambda = \frac{\Lambda\eta^{1/2}\tilde{\epsilon}^{1/2}}{K_3^{1/2}\Omega^{1/2}}, \quad \nu = \frac{\mu\tilde{\epsilon}^{1/2}}{K_3^{1/2}}, \quad \delta = \frac{d\eta^{1/2}}{K_3^{1/2}\Omega^{3/2}\tilde{\epsilon}^{1/2}} \quad (\text{II.15})$$

We then rescale all the physical quantities into dimensionless form. A tilde over a certain quantity is used to denote its dimensionless form while the reduced temperature is denoted by τ .

$$\begin{aligned} \tilde{\theta}_o &= \theta_o/\theta^* & \tilde{P}_o &= P_o/P^* \\ \tilde{q} &= q/q^* & \tilde{\chi} &= \chi/\chi^* \\ \tilde{z} &= z/z^* & \tilde{p} &= p/p^* \\ \tilde{C}_p &= C_p/C_p^* & \tilde{g} &= g/g^* \\ \tilde{E} &= E/E^* & \tau &= (T_c - T)/T^* \end{aligned} \quad (\text{II.16})$$

The characteristic units with which the quantities are scaled are denoted by using a star as a superscript. These units are defined ac-

ording to

$$\begin{aligned}
 \theta^* &= \left(\frac{1}{\bar{\epsilon}\Omega} \right)^{1/2}, & P^* &= \left(\frac{1}{\bar{\epsilon}\eta} \right)^{1/2} \\
 q^* &= \frac{1}{p^*} = \frac{1}{z^*} = \left(\frac{\Omega}{\eta\bar{\epsilon}K_3} \right)^{1/2}, & \chi^* &= \bar{\epsilon}, & T^* &= \frac{\bar{b}}{\bar{\epsilon}\alpha\Omega} \\
 g^* &= \frac{1}{\bar{\epsilon}^2\eta}, & C_\rho^* &= \frac{\alpha\Omega}{\bar{\epsilon}\eta\bar{b}}, & E^* &= \frac{1}{\bar{\epsilon}^{3/2}\eta^{1/2}}
 \end{aligned} \tag{II.17}$$

Only five of the eight scaling factors defined in Eqs. (II.17) are independent and the following three relations hold

$$g^* = \frac{P^{*2}}{\chi^*}, \quad C_\rho^* = \frac{P^{*2}}{\chi^* T^*}, \quad E^* = \frac{P^*}{\chi^*} \tag{II.18}$$

The symbol E introduced in the proceeding equations represents the electric field which we will introduce in connection to the calculation of the dielectric response. By substituting Eqs. (II.13) and (II.15)–(II.18) into Eqs. (II.14), (II.4), (II.6), (II.8) and (II.12) we can derive the dimensionless form of these equations as:

Free-energy density

$$\begin{aligned}
 \tilde{g}_o(\tilde{z}) &= \frac{1}{2}(\beta^2 - \gamma\tau)\tilde{\theta}_o^2 + \frac{1}{4}\gamma\tilde{\theta}_o^4 + \frac{1}{6}\rho\tilde{\theta}_o^6 + \frac{1}{2}\tilde{P}_o^2 \\
 &\quad - \beta\tilde{P}_o\tilde{\theta}_o - \frac{1}{2}\tilde{P}_o^2\tilde{\theta}_o^2 + \frac{1}{4}\tilde{P}_o^4 - \nu\delta\tilde{P}_o\tilde{\theta}_o^3
 \end{aligned} \tag{II.19}$$

Tilt equation

$$(\beta^2 - \gamma\tau)\tilde{\theta}_o + \gamma\tilde{\theta}_o^3 + \rho\tilde{\theta}_o^5 - \tilde{\theta}_o\tilde{P}_o^2 - (\beta + 3\nu\delta\tilde{\theta}_o^2)\tilde{P}_o = 0 \tag{II.20}$$

Polarization equation

$$\tilde{P}_o^3 + (1 - \tilde{\theta}_o^2)\tilde{P}_o - (\beta + \nu\delta\tilde{\theta}_o^2)\tilde{\theta}_o = 0 \tag{II.21}$$

Wave vector of the pitch

$$\tilde{q} = \lambda + \nu\frac{\tilde{P}_o}{\tilde{\theta}_o} + \delta\tilde{\theta}_o^2 \tag{II.22}$$

Phase transition temperature

$$T_c = T_o + \frac{T^*}{\gamma}(\beta^2 + \lambda^2) \quad (\text{II.23})$$

By introducing the scaled quantities into the definition $a = \alpha(T - T_o)$ and by using first of Eqs. (II.13) we also derive the following useful relation

$$\gamma\tau = -\frac{\tilde{a}\tilde{\epsilon}\eta}{\Omega} + \beta^2 \quad (\text{II.24})$$

We also note that by the use of Eqs. (II.15) we can derive the following useful relations between the nonrenormalized and renormalized constants of Eqs. (II.13)

$$\begin{aligned} b &= \tilde{b}\left(1 + \frac{4\lambda\delta}{\gamma}\right) & c &= \tilde{c}\left(1 + \frac{3\delta^2}{\rho}\right) \\ \frac{1}{\epsilon} &= \frac{1}{\tilde{\epsilon}}(1 + \gamma^2) & C &= \tilde{C}\left(1 - \frac{\lambda\nu}{\beta}\right) \end{aligned} \quad (\text{II.25})$$

To summarize: We have now rescaled the equations governing the tilt, polarization and pitch into dimensionless form, at the same time replacing the eleven original parameters entering Eq. (II.1) with a new set of parameters, which can conveniently be divided into two groups. Six of these parameters (Eqs. (II.13) and (II.15)) are dimensionless and are the ones which determine the shape of the calculated curves, while the other five are scaling factors which enter the calculation when converting the dimensionless quantities back to their physical correspondences. The way of writing the governing equations given by (II.20)–(II.22) will be the basic formulation which we will use when performing the calculations in this work. In Table I we have summarized the fundamental concepts of the model.

II.5 Symmetry properties of the governing equations—possible temperature dependences of the pitch

As was pointed out in Section II.1 symmetry allows four different types of ferroelectric liquid crystals. These are the combinations which can be formed by (+) and (−) substances for which the helices in turn can be either right-handed (RH) or left-handed (LH). We will denote these four types by RH(+), RH(−), LH(+) and LH(−)

TABLE I

Summary of the dimensionless, renormalized Landau model of the SmC* phase.

FREE ENERGY DENSITY				DIMENSIONLESS MODEL				EQUATIONS	
Contributing term	For small θ_0	Renormalized constants	Contribution with q eliminated	Constants	Quantity	Relation	Characteristic units	Nonrenormalized	Renormalized and dimensionless
$\frac{1}{2} \epsilon (\epsilon_1^2 + \epsilon_2^2) [s + \epsilon (T - T_0)]$	$\frac{1}{2} s \theta_0^2$	$\tilde{s} = s - \frac{1}{\epsilon_1^2}$	$\frac{1}{2} \theta_0^2$	$\gamma = \frac{\tilde{s}}{\epsilon_1^2}$	Tilt	$\tilde{\theta}_0 = \theta_0 / \theta^*$	$\theta^* = (\frac{1}{\epsilon_1})^{1/2}$	$s \theta_0^2 - 2 \Delta q \theta_0^2 + \epsilon_1 \epsilon_2 \theta_0^2 - \Delta q \theta_0^2 - \epsilon_2 \theta_0^2 - \Delta q \theta_0^2 = 0$	$(s^2 - \gamma \gamma) \theta_0^2 + \gamma \theta_0^2 + \theta_0^2 - \frac{1}{2} \theta_0^2 - (\theta + 3 \Delta q \theta_0^2) \theta_0^2 = 0$
$\frac{1}{2} 4 \epsilon (\epsilon_1^2 + \epsilon_2^2)^2$	$\frac{1}{2} 4 \theta_0^4$	$\tilde{s} = s - \frac{1}{\epsilon_1^2}$	$\frac{1}{2} 4 \theta_0^4$	$\rho = \frac{\tilde{s}}{\epsilon_1^2}$	Polarization	$\tilde{\rho}_0 = \rho / \rho^*$	$\rho^* = (\frac{1}{\epsilon_1})^{1/2}$	$\frac{1}{2} \theta_0^2 - \Delta q \theta_0^2 - \epsilon_2 \theta_0^2 - \Delta q \theta_0^2 + \theta_0^2 = 0$	$\tilde{\rho}_0^2 + (1 - \frac{3}{2} \gamma) \theta_0^2 - (\theta + \Delta q \theta_0^2) \theta_0^2 = 0$
$\frac{1}{2} \epsilon (\epsilon_1^2 + \epsilon_2^2)^3$	$\frac{1}{2} \epsilon \theta_0^6$	$\tilde{s} = s - \frac{1}{\epsilon_1^2}$	$\frac{1}{2} \epsilon \theta_0^6$	$\beta = \frac{1/2 \tilde{s}}{\epsilon_1^2}$	Pitch ($\tilde{\rho} = 2 \tilde{s} / \tilde{\rho}$)	$\tilde{\rho} = \rho / \rho^*$	$\rho^* = (\frac{1}{\epsilon_1})^{1/2}$	$q = \frac{1}{\epsilon_1} + \frac{1}{\epsilon_1} + \frac{1}{\epsilon_1} = 0$	$\tilde{q} = \lambda + \gamma + \Delta q \theta_0^2$
$\frac{1}{2} \epsilon (\epsilon_1^2 + \epsilon_2^2)^2$	$\frac{1}{2} \epsilon \theta_0^4$	$\tilde{s} = s - \frac{1}{\epsilon_1^2}$	$\frac{1}{2} \epsilon \theta_0^4$	$\lambda = \frac{1/2 \tilde{s}}{\epsilon_1^2}$	Length	$\tilde{\lambda} = \lambda / \lambda^*$	$\lambda^* = (\frac{1}{\epsilon_1})^{1/2}$		
$- A (\epsilon_1 \frac{d\epsilon_1}{dx} - \epsilon_2 \frac{d\epsilon_2}{dx})$	$- \Delta q \theta_0^2$				Free-energy density	$\tilde{\epsilon}_0 = \epsilon_0 / \epsilon^*$	$\epsilon^* = \frac{1}{\epsilon_1}$	$\epsilon_0 = \text{sum of the terms in the far left column}$	$\tilde{\epsilon}_0 = \frac{1}{2} (\beta^2 - \gamma \gamma) \theta_0^2 + \frac{1}{2} \gamma \theta_0^2 + \frac{1}{2} \theta_0^2 + \frac{1}{2} \theta_0^2 - \frac{1}{2} \theta_0^2 - \frac{1}{2} \theta_0^2 + \frac{1}{2} \theta_0^2 - \Delta q \theta_0^2$
$\frac{1}{2} \epsilon_1 (\frac{d\epsilon_1}{dx})^2 + \frac{d\epsilon_2}{dx}$	$\frac{1}{2} \epsilon_1 \theta_0^2$				Dielectric response	$\tilde{\epsilon} = \epsilon / \epsilon^*$	$\epsilon^* = \frac{1}{\epsilon_1}$		
$- \epsilon \theta_0^2 \frac{d\epsilon_1}{dx} + \epsilon_2 \frac{d\epsilon_2}{dx}$	$- \Delta q \theta_0^2$				Electric field	$\tilde{E} = E / E^*$	$E^* = \frac{1}{2 \gamma \epsilon_1^{1/2}}$	$C_p = - \frac{d^2 \epsilon_0}{dx^2} \theta_0$	$\tilde{C}_p = - (\frac{1}{\epsilon_1} - \gamma) \theta_0^2 (\frac{d^2 \epsilon_0}{dx^2})$
$- d(\epsilon_1^2 + \epsilon_2^2) (\epsilon_1 \frac{d\epsilon_1}{dx} - \epsilon_2 \frac{d\epsilon_2}{dx})$	$- \epsilon \theta_0^4$				Max capacity	$\tilde{C}_p = C_p / C^*$	$C^* = \frac{1}{\epsilon_1}$	$T_c = T_0 + \frac{1}{2} (\frac{1}{\epsilon_1} - \frac{1}{\epsilon_1})^2$	$T_c = T_0 + \frac{1}{2} [\beta^2 + \lambda^2]$
$\epsilon \theta_0^2 \epsilon_1 - \epsilon_2 \epsilon_1$	$- \epsilon \theta_0^2$				Temperature	$\tilde{T} = T / T^*$	$T^* = \frac{1}{\epsilon_1}$		
$-\frac{1}{2} \Delta q \epsilon_1 \epsilon_2 - \epsilon_2 \epsilon_1^2$	$-\frac{1}{2} \Delta q \theta_0^2$								
$\frac{1}{2} \epsilon (\epsilon_1^2 + \epsilon_2^2)^2$	$\frac{1}{2} \epsilon \theta_0^4$								

respectively. It was also noted in Section II.1 that while we could assume seven of the constants entering the Landau expansion of the free energy density to be positive, the signs of the four constants Λ , d , μ and C are arbitrary. By changing the signs of these four constants in all possible ways we arrive at sixteen different combinations. Each such combination will be denoted by us as a state. In this section we will investigate in which way these sixteen states are connected to the four different types of ferroelectric liquid crystals that symmetry allows. As there is a one to one correspondence between the signs of the four constants Λ , d , μ and C and the signs of the four dimensionless parameters λ , δ , ν and β (Eqs. II.15)), the result of this section can directly be transferred into the dimensionless model by the substitutions $\Lambda \rightarrow \lambda$, $d \rightarrow \delta$, $\mu \rightarrow \nu$ and $C \rightarrow \beta$.

As we will notice, for some states our model predicts q to change sign at some temperature, describing a transformation from a RH to a LH type of helix. We also will show in Section III.3 how, under some circumstances, our model predicts the polarization to change sign with temperature. Due to these facts we will classify the states according to their behaviour at T_c . From Eqs. (II.4) and (II.11) we derive $q(T = T_c) \equiv q_o$ to be

$$q_o = \frac{1}{K_3} \left(\Lambda + \mu \frac{\Lambda\mu/K_3 + C}{1/\epsilon - \mu^2/K_3} \right) = \frac{\Lambda + \epsilon\mu C}{K_3 - \epsilon\mu^2} \quad (\text{II.26})$$

For a RH state, q_o shall be positive leading to the inequality ($K_3 - \epsilon\mu^2$ must be positive by stability reasons)

$$\Lambda + \mu C \epsilon > 0 \quad (\text{II.27})$$

The condition for the compound to be of RH or LH type which can be derived from Eq. (II.27) will of course depend not only on the signs of the ingoing parameters but also of their relative magnitude. Knowing however that the polarization of the system is a weak second order effect, we will assume that the renormalization of Λ which is implied by Eq. (II.27), is not large enough to change its sign. Within this limitation, it is thus clear that a positive Λ corresponds to a RH type and a negative Λ to a LH type of helix. Concerning the sign of the polarization at T_c we study Eq. (II.21). From this we conclude that $\lim_{\tau \rightarrow 0} \tilde{P}_o = \beta \tilde{\theta}_o$. As $\tilde{\theta}_o$ is taken to be positive by definition, we thus conclude that close to T_c the sign of the polarization is the same as the sign of β . From the definition of β (Eqs. (II.13) and (II.15))

we thus conclude that it is the sign of $\tilde{C} = C + \Lambda\mu/K_3$ which determines whether a compound is of (+) or (−) type. Assuming that we are dealing with a system of weak chirality, the renormalization of C will not be large enough to change its sign and we conclude that (+) substances correspond to positive C while (−) substances correspond to negative C .

In Figure 2 we have expressed the sixteen different states which can occur in terms of the signs of the four constants Λ , d , μ and C . We find four states corresponding to each of the four types RH(+), RH(−), LH(+) and LH(−). Within the approximations of weak polarization and chirality made above, the signs of Λ and C determine to which type each state will belong. A compound can exist in one of its two racemic forms, which is either RH or LH. Also, symmetry requires that the two racemics should have opposite signs of polarization. This means that the governing equations of the system must be invariant by the transformations which takes RH(+) into LH(−) and LH(+) into RH(−) and vice versa. We now derive the set of transformations which leave the set of Eqs. (II.5)–(II.8) invariant.

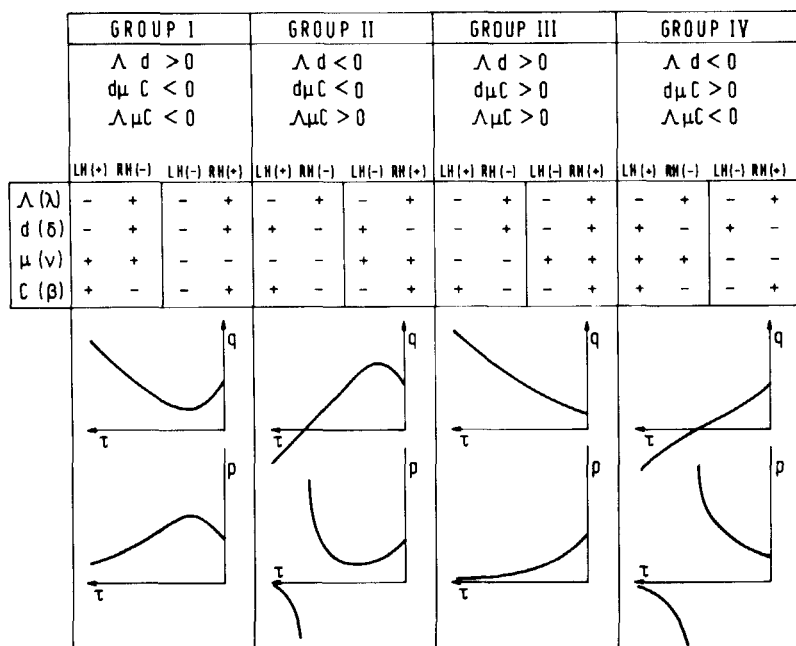


FIGURE 2 The sixteen possible states with respect to the sign of the parameters $\Lambda(\lambda)$, $d(\delta)$, $\mu(\nu)$ and $C(\beta)$ and the corresponding behaviour of the pitch. The type of each state is indicated in the figure in the limit $|\Lambda| > \epsilon|\mu C|$ and $|C| > |\Lambda\mu|/K_3$.

Demanding the invariance of the term $(b - 4\Lambda d/K_3)\theta_o^3$ implies sign (Λd) to be invariant. Further on the invariance of the term $3d\mu\theta_o^2P_o/K_3$ implies sign $(d\mu P_o) = \text{sign}(d\mu C)$ to be invariant. A corollary of these two rules is that sign $(\Lambda\mu C)$ shall be invariant under the transformations, a fact which also follows from the invariance of the term $(C + \Lambda\mu/K_3)P_o$. In this way we have divided the sixteen states into four groups containing one state each of the four types RH(+), LH(+), RH(-) and LH(-). For the four states within each group sign (Λd) , sign $(d\mu C)$ and sign $(\Lambda\mu C)$ are invariant, implying that all physical properties of the states are identical except concerning the change of signs of q_o and P_o . Within each group there exist three transformations which bring the four states into each other:

- 1) Change of sign of q and P_o —"the racemic transformation"
($\Lambda \rightarrow -\Lambda$, $d \rightarrow -d$, $\mu \rightarrow \mu$, $C \rightarrow -C$)
- 2) Change of sign P_o only ($\Lambda \rightarrow \Lambda$, $d \rightarrow d$, $\mu \rightarrow -\mu$, $C \rightarrow -C$)
- 3) Change of sign of q only ($\Lambda \rightarrow -\Lambda$, $d \rightarrow -d$, $\mu \rightarrow -\mu$, $C \rightarrow C$).

The behaviour of the pitch is qualitatively different between the four groups as is seen in Figure 2, where we have plotted q and p as functions of temperature for the RH states, assuming $|\beta| < 1$ and $|\delta| < |\beta|$. These assumptions will be justified in Section III.5. Within two groups ($d\mu C < 0$) q exhibits an extremum, while within the other two groups ($d\mu C > 0$) q increases or decreases monotonously. Furtheron, within two of the groups ($\Lambda d < 0$) q goes through zero implying a transition from a right-handed to a left-handed helix or vice versa. For the states belonging to groups I and IV ($\Lambda\mu C < 0$) a strong renormalization of Λ would force $\Lambda + \epsilon\mu C$ to change sign. The behaviour of the pitch belonging to group I would then be transformed into the behaviour of group II, while the pitch of group IV would be transformed into the behaviour of group III. We also note concerning the states belonging to group I, that for an intermediate strong renormalization of Λ , i.e. if $|\Lambda + \epsilon\mu C|$ is small enough to permit the maximum (minimum) of q to have a different sign than q_o , the pitch will change sign twice as function of temperature. The behaviour of the pitch of the states belonging to group I in the three different cases discussed above is shown in Figure 3. The five different types of pitches which are shown in Figures 2 and 3 are the only ones which are permitted by our model (if $|\beta| < 1$ and $|\delta| < |\beta|$).

We thus have established a way to determine the signs of all the parameters in the free-energy density of our model provided that we investigate the behaviour of the pitch and the strength of the renor-

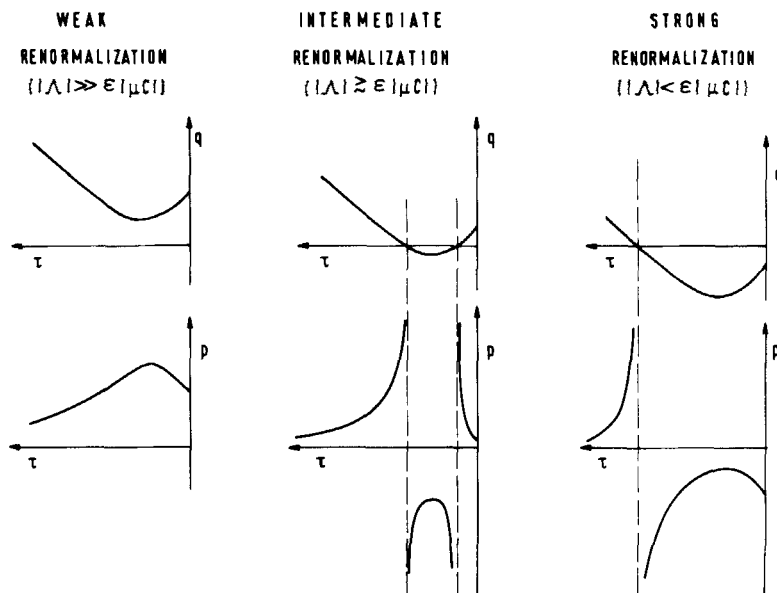


FIGURE 3 The behaviour of the pitch of the states belonging to group I in the cases of weak, intermediate and strong renormalization of the Lifshitz coefficient Λ .

malization of Λ . The shape of the pitch which is usually experimentally reported, is the one which corresponds to group I of Figure 2. The only possibility of achieving this behaviour is to use one of the states of group I in the limit $|\Lambda| \gg \epsilon |\mu C|$, i.e. the experimental behaviour of the pitch confirms our starting assumption of weak renormalization of Λ . Knowing to which of the four possible types RH(+), RH(-), LH(+) or LH(-) the liquid crystal with which we are dealing belongs, we thus can determine the signs of the four constants Λ , d , μ and C unambiguously.

II.6 Unwinding of the helix

Solving the equations (II.20)–(II.22) will give the tilt, the polarization and the pitch of an undisturbed SmC* liquid crystal. One important task is then to experimentally determine the six constants (Eqs. (II.15)) entering into these equations. Sometimes however, the experiments are not being performed by using the liquid crystal in its ground state, but by using an unwound sample, where the pitch is made infinitely long by the application of some external force (induced SmC phase—“the homogeneous case”). It is therefore of interest to know how this unwinding affects quantities such as tilt and polarization. In this

section we will show, how one can derive equations governing these quantities in the homogeneous case which are having the same structure as the previously derived ones. This will enable us to compare calculations and experiments, performed in the two cases, in a simple manner.

In the homogeneous case we will find it natural to introduce another scaling in contrast to the one which is defined by Eqs. (II.16) and (II.17). We will denote the scaled tilt, polarization, free-energy density and the reduced temperature according to

$$\begin{aligned}\tilde{\theta}_h &= \theta_o/\theta_h^* & \tilde{P}_h &= P_o/P_h^* \\ \tilde{g}_h &= g_o/g_h^* & \tau_h &= (T_{ch} - T)/T_h^*\end{aligned}\quad (\text{II.28})$$

where T_{ch} is the phase transition temperature in the homogeneous case. The characteristic units which are introduced in Eqs. (II.28) are defined as

$$\begin{aligned}\theta_h^* &= \left(\frac{1}{\epsilon\Omega}\right)^{1/2} = \theta^* (1 + \nu^2)^{1/2} \\ P_h^* &= \left(\frac{1}{\epsilon\eta}\right)^{1/2} = P^* (1 + \nu^2)^{1/2} \\ g_h^* &= \frac{1}{\epsilon^2\eta} = g^* (1 + \nu^2)^2 \\ T_h^* &= \frac{b}{\epsilon\alpha\Omega} = T^* (1 + \nu^2) \left(1 + \frac{4\lambda\delta}{\gamma}\right)\end{aligned}\quad (\text{II.29})$$

The right hand side of Eqs. (II.29) can be derived by using Eqs. (II.17) and (II.25).

In the homogeneous case q is zero and we can write the free-energy density of Eq. (II.3) as

$$\begin{aligned}g_o(q = 0) &= \frac{1}{2}a\theta_o^2 + \frac{1}{4}b\theta_o^4 + \frac{1}{6}c\theta_o^6 + \frac{1}{2\epsilon}P_o^2 \\ &\quad - CP_o\theta_o - \frac{1}{2}\Omega P_o^2\theta_o^2 + \frac{1}{4}\eta P_o^4\end{aligned}\quad (\text{II.30})$$

By rewriting this equation into dimensionless form, using the scaling

introduced in Eqs. (II.28) and (II.29) and also by using the equalities (II.25) we get

$$\begin{aligned}\bar{g}_h = & \frac{1}{2} \frac{a\eta\bar{\epsilon}}{\Omega} \frac{\bar{\theta}_h^2}{1 + \nu^2} + \frac{1}{4} \left(1 + \frac{4\lambda\delta}{\gamma} \right) \gamma \bar{\theta}_h^4 \\ & + \frac{1}{6} \left(1 + \frac{3\delta^2}{\rho} \right) (1 + \nu^2) \rho \bar{\theta}_h^6 + \frac{1}{2} \bar{P}_h^2 - \frac{1 - \frac{\lambda\nu}{\beta}}{1 + \nu^2} \beta \bar{P}_h \bar{\theta}_h \\ & - \frac{1}{2} \bar{P}_h^2 \bar{\theta}_h^2 + \frac{1}{4} \bar{P}_h^4\end{aligned}\quad (\text{II.31})$$

We now write the equations in the homogeneous case in the same form as they were written in the nonhomogeneous case. Apart from the new scaling defined by Eqs. (II.28) and (II.29) we also will have to redefine the constants of Eqs. (II.15). We will denote them γ_h , β_h , ρ_h , δ_h , ν_h and λ_h in the homogeneous case. The free-energy density of Eq. (II.19) is then written

$$\begin{aligned}\bar{g}_h = & \frac{1}{2} (\beta_h^2 - \gamma_h \tau_h) \bar{\theta}_h^2 + \frac{1}{4} \gamma_h \bar{\theta}_h^4 + \frac{1}{6} \rho_h \bar{\theta}_h^6 + \frac{1}{2} \bar{P}_h^2 \\ & - \beta_h \bar{P}_h \bar{\theta}_h - \frac{1}{2} \bar{P}_h^2 \bar{\theta}_h^2 + \frac{1}{4} \bar{P}_h^4 - \nu_h \delta_h \bar{\theta}_h^3 \bar{P}_h\end{aligned}\quad (\text{II.32})$$

By comparing Eqs. (II.31) and (II.32) we get

$$\begin{aligned}\beta_h^2 - \gamma_h \tau_h &= \frac{a\eta\bar{\epsilon}}{\Omega} \frac{1}{1 + \nu^2} \\ \gamma_h &= \left(1 + \frac{4\lambda\delta}{\gamma} \right) \gamma \\ \rho_h &= \left(1 + \frac{3\delta^2}{\rho} \right) (1 + \nu^2) \rho \\ \beta_h &= \frac{1 - \frac{\lambda\nu}{\beta}}{1 + \nu^2} \beta \\ \nu_h \delta_h &= 0\end{aligned}\quad (\text{II.33})$$

The wave vector of the pitch, which in the homogeneous case is zero, gives rise to the following relation (c.f. Eq. (II.22))

$$\bar{q}_h = \lambda_h + \nu_h \frac{\bar{P}_h}{\bar{\theta}_h} + \delta_h \theta_h^2 \equiv 0 \quad (\text{II.34})$$

which demands

$$\lambda_h = \nu_h = \delta_h = 0 \quad (\text{II.35})$$

In Eqs. (II.33) and (II.35) we have established the relations between the constants as they appear in the homogeneous case and the relaxed, undisturbed state, respectively. Concerning the reduced temperature and the SmC*-SmA phase transition temperature in the unwound case, T_{ch} , we can derive from Eqs. (II.23), (II.24) and (II.33) the following relations

$$\tau_h = \frac{\tau}{(1 + \nu^2) \left(1 + \frac{4\lambda\delta}{\nu}\right)} - \frac{\nu^2 \beta^2}{\gamma} \frac{\left(1 + \frac{\lambda}{\nu\beta}\right)^2}{(1 + \nu^2)^2 \left(1 + \frac{4\lambda\delta}{\gamma}\right)}$$

$$T_{ch} = T_o + \frac{T^* \beta^2}{\gamma} \frac{\left(1 - \frac{\lambda\nu}{\beta}\right)^2}{1 + \nu^2} \quad (\text{II.36})$$

The equations governing the tilt and the polarization in the homogeneous case can now be obtained from Eq. (II.32) by minimizing g_h with respect to $\bar{\theta}_h$ and \bar{P}_h and we get:

Tilt equation in the homogeneous case

$$(\beta_h^2 - \gamma_h \tau_h) \bar{\theta}_h + \gamma_h \bar{\theta}_h^3 + \rho_h \bar{\theta}_h^5 - \bar{\theta}_h \bar{P}_h^2 - \beta_h \bar{P}_h = 0 \quad (\text{II.37})$$

Polarization equation in the homogeneous case

$$\bar{P}_h^3 + (1 - \bar{\theta}_h^2) \bar{P}_h - \beta_h \bar{\theta}_h = 0 \quad (\text{II.38})$$

By comparing these equations with Eqs. (II.20) and (II.21) we confirm that the structure of the equations is the same in the two cases. What we have achieved is that after having determined the material parameters entering the equations in one of the two cases we immediately can transfer these values to the other case. We should

however be aware of that not only the constants, but also the scaling differs according to Eq. (II.29). Also the phase transition temperature is shifted according to the last of Eqs. (II.36). In Section III.2 we will show that the values of the material parameters are such, that most of the corrections entering into Eqs. (II.29) and (II.36) are negligible.

II.7 The static dielectric susceptibility

As was discussed in the introduction, the spontaneous polarization of the SmC* phase precesses helicoidally as the medium is crossed perpendicular to the smectic layers. Thus we see that even if the system exhibits a local net polarization, the macroscopic average of this will be zero. Applying an electric field of magnitude E parallel to the smectic layers will however disturb the helix in such a way that an average macroscopic polarization $\langle P_i \rangle$ is induced. The dielectric susceptibility χ is then defined as

$$\chi = \lim_{E \rightarrow 0} \frac{\langle P_i \rangle}{E} \quad (\text{II.39})$$

Without loss of generality we assume the electric field to be given by

$$\mathbf{E} = E\hat{x} \quad (\text{II.40})$$

This field will add to the free-energy density of Eq. (II.1) an extra contribution given by

$$g_E = -\mathbf{E} \cdot \mathbf{P} = -EP_x \quad (\text{II.41})$$

The total free-energy density of the system is now given by the sum of Eqs. (II.1) and (II.41). In order to calculate this we again will have to make an ansatz for the order parameters ξ and \mathbf{P} . The helicoidal ansatz of Eqs. (II.2) will not any longer be correct, since this referred to a system with an undisturbed helix. The applied electric field will however disturb the helix in two ways. First of all the tilt of the molecules will change and secondly the molecules will rotate slightly in order to align the local polarization along the field. In this way both the amplitude and the phase of the order parameters ξ and \mathbf{P} will be influenced by the field. Denoting the amplitude changes by $\delta\theta_1$ and δP_1 and the phase changes by $\delta\theta_2$ and δP_2 , respectively, we

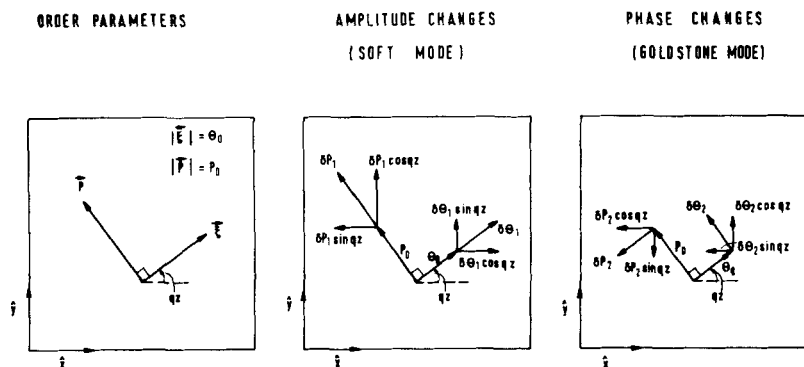


FIGURE 4 The order parameters ξ and \mathbf{P} and their changes due to the application of an electric field parallel to the smectic layers. The amplitude changes, which are connected to the soft mode, are denoted $\delta\theta_1$ and δP_1 while the phase changes, which are connected to the Goldstone mode, are denoted $\delta\theta_2$ and δP_2 .

see from Figure 4 that ξ and \mathbf{P} can be written

$$\xi_1 = \theta_0 \cos qz + \delta\theta_1 \cos qz - \delta\theta_2 \sin qz$$

$$\xi_2 = \theta_0 \sin qz + \delta\theta_1 \sin qz + \delta\theta_2 \cos qz$$

$$P_x = -P_0 \sin qz - \delta P_1 \sin qz - \delta P_2 \cos qz$$

$$P_y = P_0 \cos qz + \delta P_1 \cos qz - \delta P_2 \sin qz \quad (\text{II.42})$$

In this way we have divided the dielectric response into two modes, one which is due to amplitude changes (soft mode) and one which is due to phase changes (Goldstone mode) of the order parameter. This division is however not clear-cut due to a small amplitude-phase coupling: the part which corresponds to the amplitude changes in \mathbf{P} mostly corresponds to the amplitude changes in ξ , but also induces a small phase contribution in the tilt. We will show in Section III.6 that this coupling is so small, that we as a good approximation† can

†In order to derive the expressions of the eigenmodes of the system rigorously we have to study the dynamical response of the system. Such derivation has been performed by us recently and has been submitted in February 1988 for publication to the Physical Review A.

define the two modes as

$$\begin{aligned}\chi_1 &= \lim_{E \rightarrow 0} \frac{\langle P_{i1} \rangle}{E} \quad (\text{Soft mode}) \\ \chi_2 &= \lim_{E \rightarrow 0} \frac{\langle P_{i2} \rangle}{E} \quad (\text{Goldstone mode})\end{aligned} \quad (\text{II.43})$$

where $\langle P_{i1} \rangle$ and $\langle P_{i2} \rangle$ are the averages of the amplitude part and the phase part of the induced polarization, respectively.

Introducing the ansatz (II.42) into Eqs. (II.1) and (II.41), we can write the total free-energy density to second order in $\delta\theta$ and δP as

$$g(z) = g_o(z) + g_1(z) + g_2(z) + g_E(z) \quad (\text{II.44})$$

where $g_o(z)$ is already given by Eq. (II.3). Letting a prime denote a space derivative with respect to z (i.e. $\delta\theta'_i \equiv d(\delta\theta_i)/dz$ and so on) we get

$$\begin{aligned}g_1(z) &= \delta\theta_1(a\theta_o + b\theta_o^3 + c\theta_o^5 - 2\Lambda q\theta_o + K_3q^2\theta_o - \mu qP_o \\ &\quad - CP_o - \Omega P_o^2\theta_o - 4dq\theta_o^3) \\ &\quad + \delta P_1 \left(\frac{1}{\epsilon} P_o - \mu q\theta_o - C\theta_o - \Omega P_o\theta_o^2 + \eta P_o^3 \right) \\ &\quad + \delta\theta'_2 (-\Lambda\theta_o + K_3q\theta_o - \mu P_o - d\theta_o^3) \equiv 0\end{aligned} \quad (\text{II.45})$$

As $g(z)$ is expanded around a minimum $g_1(z)$ vanishes identically, a fact which can also be confirmed by Eqs. (II.4), (II.5) and (II.7). Further on we get

$$\begin{aligned}g_2(z) &= \delta\theta_1^2 \left(\frac{1}{2}a + \frac{3}{2}b\theta_o^2 + \frac{5}{2}c\theta_o^4 - \Lambda q + \frac{1}{2}K_3q^2 - \frac{1}{2}\Omega P_o^2 \right. \\ &\quad \left. - 6dq\theta_o^2 \right) \\ &\quad + \delta\theta_2^2 \left(\frac{1}{2}a + \frac{1}{2}b\theta_o^2 + \frac{1}{2}c\theta_o^4 - \Lambda q + \frac{1}{2}K_3q^2 - 2dq\theta_o^2 \right) \\ &\quad + \delta P_1^2 \left(\frac{1}{2\epsilon} - \frac{1}{2}\Omega\theta_o^2 + \frac{3}{2}\eta P_o^2 \right)\end{aligned}$$

$$\begin{aligned}
& + \delta P_2^2 \left(\frac{1}{2\epsilon} + \frac{1}{2} \eta P_o^2 \right) \\
& - \delta \theta_1 \delta P_1 (\mu q + C + 2\Omega P_o \theta_o) \\
& - \delta \theta_2 \delta P_2 (\mu q + C + \Omega P_o \theta_o) \\
& + \delta \theta_1 \delta \theta_2' (-\Lambda + K_3 q - 3d\theta_o^2) \\
& + \delta \theta_1' \delta \theta_2 (\Lambda - K_3 q + d\theta_o^2) \\
& + \frac{1}{2} K_3 (\delta \theta_1'^2 + \delta \theta_2'^2) + \mu (\delta P_2 \delta \theta_1' - \delta P_1 \delta \theta_2')
\end{aligned} \tag{II.46}$$

and

$$g_E(z) = E(P_o \sin qz + \delta P_1 \sin qz + \delta P_2 \cos qz) \tag{II.47}$$

The total free energy of the system, which is given by

$$G = A \int_0^L [g_o(z) + g_2(z) + g_E(z)] dz \tag{II.48}$$

where A is the area and L the thickness of the sample perpendicular to smectic layers, has now to be minimized. The contribution from $g_o(z)$ to the integral is just a constant and does not have to be considered. By applying the Euler-Lagrange equations we know that the configuration $\delta \theta_1(z)$, $\delta \theta_2(z)$, $\delta P_1(z)$ and $\delta P_2(z)$ which minimizes the integral (II.48) is given by (in Eqs. (II.49) we use $g \equiv g_2 + g_E$ for the sake of simplicity)

$$\begin{aligned}
\frac{\partial g}{\partial \delta \theta_1} - \frac{d}{dz} \frac{\partial g}{\partial \delta \theta_1'} &= 0 \\
\frac{\partial g}{\partial \delta \theta_2} - \frac{d}{dz} \frac{\partial g}{\partial \delta \theta_2'} &= 0 \\
\frac{\partial g}{\partial \delta P_1} - \frac{d}{dz} \frac{\partial g}{\partial \delta P_1'} &= 0 \\
\frac{\partial g}{\partial \delta P_2} - \frac{d}{dz} \frac{\partial g}{\partial \delta P_2'} &= 0
\end{aligned} \tag{II.49}$$

By substituting Eqs. (II.46) and (II.47) into Eqs. (II.49) we finally get

$$\begin{aligned}
 & K_3 \delta \theta_1'' + (2\Lambda - 2K_3 q + 4d\theta_o^2) \delta \theta_2' + \mu \delta P_2' - (a + 3b\theta_o^2 + 5c\theta_o^4 - 2\Lambda q \\
 & \quad + K_3 q^2 - \Omega P_o^2 - 12dq\theta_o^2) \delta \theta_1 + (\mu q + C + 2\Omega P_o \theta_o) \delta P_1 = 0 \\
 & K_3 \delta \theta_2'' - (2\Lambda - 2K_3 q + 4d\theta_o^2) \delta \theta_1' - \mu \delta P_1' - (a + b\theta_o^2 + c\theta_o^4 \\
 & \quad - 2\Lambda q + K_3 q^2 - 4dq\theta_o^2) \delta \theta_2 + (\mu q + C + \Omega P_o \theta_o) \delta P_2 = 0 \\
 & - \mu \delta \theta_2' - (\mu q + C + 2\Omega P_o \theta_o) \delta \theta_1 \\
 & \quad + \left(\frac{1}{\epsilon} - \Omega \theta_o^2 + 3\eta P_o^2 \right) \delta P_1 = -E \sin qz \\
 & \mu \delta \theta_1' - (\mu q + C + \Omega P_o \theta_o) \delta \theta_2 + \left(\frac{1}{\epsilon} + \eta P_o^2 \right) \delta P_2 = -E \cos qz
 \end{aligned} \tag{II.50}$$

We now make the following ansatz for the space variation of $\delta \theta$ and δP

$$\begin{aligned}
 \delta \theta_1(z) &= \delta \theta_{11} \cos qz + \delta \theta_{10} \sin qz \\
 \delta \theta_2(z) &= \delta \theta_{20} \cos qz + \delta \theta_{21} \sin qz \\
 \delta P_1(z) &= \delta P_{11} \cos qz + \delta P_{10} \sin qz \\
 \delta P_2(z) &= \delta P_{20} \cos qz + \delta P_{21} \sin qz
 \end{aligned} \tag{II.51}$$

where $\delta \theta_{ij}$ and δP_{ij} give the magnitudes of the changes while their space variation is contained in the $\cos qz$ and $\sin qz$ terms. Introducing Eqs. (II.51) into Eqs. (II.50) we derive the following algebraic equations for $\delta \theta_{ij}$ and δP_{ij}

$$\begin{aligned}
 \delta \theta_{11} &= \delta \theta_{21} = 0 \\
 \delta P_{11} &= \delta P_{21} = 0
 \end{aligned} \tag{II.52}$$

and

$$\begin{aligned}
 b_1 \delta \theta_{10} + b_2 \delta \theta_{20} + b_3 \delta P_{10} + b_4 \delta P_{20} &= 0 \\
 b_2 \delta \theta_{10} + b_5 \delta \theta_{20} + b_4 \delta P_{10} + b_6 \delta P_{20} &= 0 \\
 -b_3 \delta \theta_{10} - b_4 \delta \theta_{20} + b_7 \delta P_{10} &= -E \\
 -b_4 \delta \theta_{10} - b_6 \delta \theta_{20} + b_8 \delta P_{20} &= -E \quad (\text{II.53})
 \end{aligned}$$

where coefficients b_i are given by

$$\begin{aligned}
 b_1 &= -a - 3b\theta_o^2 - 5c\theta_o^4 + 2\Lambda q - 2q^2 K_3 + \Omega P_o^2 + 12dq\theta_o^2 \\
 b_2 &= -2\Lambda q + 2q^2 K_3 - 4dq\theta_o^2 \\
 b_3 &= \mu q + C + 2\Omega P_o \theta_o \\
 b_4 &= -\mu q \\
 b_5 &= -a - b\theta_o^2 - c\theta_o^4 + 2\Lambda q - 2q^2 K_3 + 4dq\theta_o^2 \\
 b_6 &= \mu q + C + \Omega P_o \theta_o \\
 b_7 &= \frac{1}{\epsilon} - \Omega \theta_o^2 + 3\eta P_o^2 \\
 b_8 &= \frac{1}{\epsilon} + \eta P_o^2 \quad (\text{II.54})
 \end{aligned}$$

As was pointed out in Section II.4 the equations governing the behaviour of the system are most conveniently given in dimensionless form. We now once more introduce the scaling defined by Eqs. (II.16) and (II.17)

$$\begin{aligned}
 \widetilde{\delta \theta}_1 &= \frac{\delta \theta_{10}}{\theta^*}, & \widetilde{\delta \theta}_2 &= \frac{\delta \theta_{20}}{\theta^*} \\
 \widetilde{\delta P}_1 &= \frac{\delta P_{10}}{P^*}, & \widetilde{\delta P}_2 &= \frac{\delta P_{20}}{P^*} \quad (\text{II.55})
 \end{aligned}$$

Eqs. (II.53) now transform into

$$\begin{aligned}
 \tilde{b}_1 \tilde{\delta} \tilde{\theta}_1 + \tilde{b}_2 \tilde{\delta} \tilde{\theta}_2 + \tilde{b}_3 \tilde{\delta} \tilde{P}_1 + \tilde{b}_4 \tilde{\delta} \tilde{P}_2 &= 0 \\
 \tilde{b}_2 \tilde{\delta} \tilde{\theta}_1 + \tilde{b}_5 \tilde{\delta} \tilde{\theta}_2 + \tilde{b}_4 \tilde{\delta} \tilde{P}_1 + \tilde{b}_6 \tilde{\delta} \tilde{P}_2 &= 0 \\
 -\tilde{b}_3 \tilde{\delta} \tilde{\theta}_1 - \tilde{b}_4 \tilde{\delta} \tilde{\theta}_2 + \tilde{b}_7 \tilde{\delta} \tilde{P}_1 &= -\tilde{E} \\
 -\tilde{b}_4 \tilde{\delta} \tilde{\theta}_1 - \tilde{b}_6 \tilde{\delta} \tilde{\theta}_2 + \tilde{b}_8 \tilde{\delta} \tilde{P}_2 &= -\tilde{E} \quad (\text{II.56})
 \end{aligned}$$

where the dimensionless coefficients \tilde{b}_i are given by

$$\begin{aligned}
 \tilde{b}_1 &= -\beta^2 + \gamma\tau - \lambda^2 - (2\lambda\delta + 3\gamma)\tilde{\theta}_o^2 - 5\rho\tilde{\theta}_o^4 + \tilde{P}_o^2 \\
 &\quad + 8\nu\tilde{P}_o\tilde{\theta}_o - 2\lambda\nu\tilde{P}_o/\tilde{\theta}_o - 2\nu^2(\tilde{P}_o/\tilde{\theta}_o)^2 - 5\delta^2\tilde{\theta}_o^4 \\
 \tilde{b}_2 &= -2\lambda\delta\tilde{\theta}_o^2 - 2\delta^2\tilde{\theta}_o^4 + 2\lambda\nu\tilde{P}_o/\tilde{\theta}_o + 2\nu^2(\tilde{P}_o/\tilde{\theta}_o)^2 \\
 \tilde{b}_3 &= \beta + \nu\delta\tilde{\theta}_o^2 + 2\tilde{P}_o\tilde{\theta}_o + \nu^2\tilde{P}_o/\tilde{\theta}_o \\
 \tilde{b}_4 &= -[\lambda\nu + \nu^2\tilde{P}_o/\tilde{\theta}_o + \nu\delta\tilde{\theta}_o^2] \\
 \tilde{b}_5 &= -\beta^2 + \gamma\tau - \lambda^2 - (2\lambda\delta + \gamma)\tilde{\theta}_o^2 - \rho\tilde{\theta}_o^4 \\
 &\quad - \delta^2\tilde{\theta}_o^4 - 2\lambda\nu\tilde{P}_o/\tilde{\theta}_o - 2\nu^2(\tilde{P}_o/\tilde{\theta}_o)^2 \\
 \tilde{b}_6 &= \beta + \nu\delta\tilde{\theta}_o^2 + \tilde{P}_o\tilde{\theta}_o + \nu^2\tilde{P}_o/\tilde{\theta}_o \\
 \tilde{b}_7 &= 1 + \nu^2 + 3\tilde{P}_o^2 - \tilde{\theta}_o^2 \\
 \tilde{b}_8 &= 1 + \nu^2 + \tilde{P}_o^2 \quad (\text{II.57})
 \end{aligned}$$

The solution of Eqs. (II.56) can be written

$$\begin{aligned}
 \tilde{\delta} \tilde{\theta}_1 &= \frac{\tilde{E}}{A} \{ -\tilde{b}_2 \tilde{b}_4 \tilde{b}_8 - \tilde{b}_2 \tilde{b}_6 \tilde{b}_7 - \tilde{b}_3 \tilde{b}_4 \tilde{b}_6 + \tilde{b}_3 \tilde{b}_5 \tilde{b}_8 \\
 &\quad + \tilde{b}_3 \tilde{b}_6^2 + \tilde{b}_4^3 + \tilde{b}_4 \tilde{b}_5 \tilde{b}_7 - \tilde{b}_4^2 \tilde{b}_6 \}
 \end{aligned}$$

$$\begin{aligned}
\tilde{\delta\theta}_2 &= \frac{\tilde{E}}{A} \{ \tilde{b}_1 \tilde{b}_4 \tilde{b}_8 + \tilde{b}_1 \tilde{b}_6 \tilde{b}_7 - \tilde{b}_2 \tilde{b}_3 \tilde{b}_8 - \tilde{b}_2 \tilde{b}_4 \tilde{b}_7 \\
&\quad - \tilde{b}_3 \tilde{b}_4^2 - \tilde{b}_3 \tilde{b}_4 \tilde{b}_6 + \tilde{b}_3^2 \tilde{b}_6 + \tilde{b}_4^3 \} \\
\tilde{\delta P}_1 &= \frac{\tilde{E}}{A} \{ \tilde{b}_1 \tilde{b}_4 \tilde{b}_6 - \tilde{b}_1 \tilde{b}_5 \tilde{b}_8 - \tilde{b}_1 \tilde{b}_6^2 - \tilde{b}_2 \tilde{b}_3 \tilde{b}_6 - \tilde{b}_2 \tilde{b}_4^2 \\
&\quad + 2 \tilde{b}_2 \tilde{b}_4 \tilde{b}_6 + \tilde{b}_2^2 \tilde{b}_8 + \tilde{b}_3 \tilde{b}_4 \tilde{b}_5 - \tilde{b}_4^2 \tilde{b}_5 \} \\
\tilde{\delta P}_2 &= \frac{\tilde{E}}{A} \{ -\tilde{b}_1 \tilde{b}_4^2 + \tilde{b}_1 \tilde{b}_4 \tilde{b}_6 - \tilde{b}_1 \tilde{b}_5 \tilde{b}_7 + 2 \tilde{b}_2 \tilde{b}_3 \tilde{b}_4 - \tilde{b}_2 \tilde{b}_3 \tilde{b}_6 \\
&\quad - \tilde{b}_2 \tilde{b}_4^2 + \tilde{b}_2^2 \tilde{b}_7 + \tilde{b}_3 \tilde{b}_4 \tilde{b}_5 - \tilde{b}_3^2 \tilde{b}_5 \}
\end{aligned} \tag{II.58}$$

where

$$\begin{aligned}
A &= \tilde{b}_1 \tilde{b}_4^2 \tilde{b}_8 + \tilde{b}_1 \tilde{b}_5 \tilde{b}_7 \tilde{b}_8 + \tilde{b}_1 \tilde{b}_6^2 \tilde{b}_7 - 2 \tilde{b}_2 \tilde{b}_3 \tilde{b}_4 \tilde{b}_8 \\
&\quad - 2 \tilde{b}_2 \tilde{b}_4 \tilde{b}_6 \tilde{b}_7 - \tilde{b}_2^2 \tilde{b}_7 \tilde{b}_8 - 2 \tilde{b}_3 \tilde{b}_4^2 \tilde{b}_6 + \tilde{b}_3^2 \tilde{b}_5 \tilde{b}_8 \\
&\quad + \tilde{b}_3^2 \tilde{b}_6^2 + \tilde{b}_4^4 + \tilde{b}_4^2 \tilde{b}_5 \tilde{b}_7
\end{aligned} \tag{II.59}$$

We now calculate the average polarization of the sample by using Eqs. (II.42), (II.51) and (II.52)

$$\begin{aligned}
\langle P_x \rangle &= \langle -P_o \sin qz \rangle - \langle \delta P_{10} \sin^2 qz \rangle - \langle \delta P_{20} \cos^2 qz \rangle \\
&= -1/2(\delta P_{10} + \delta P_{20}) \\
\langle P_y \rangle &= \langle P_o \cos qz \rangle + \langle \delta P_{10} \sin qz \cos qz \rangle \\
&\quad - \langle \delta P_{20} \sin qz \cos qz \rangle = 0
\end{aligned} \tag{II.60}$$

The dielectric response, $\tilde{\chi}$, in its scaled version is now given by substituting Eqs. (II.60) into Eqs. (II.39) (as the average polarization is zero when the electric field is switched off the average induced polarization equals the average polarization in the presence of the field)

$$\tilde{\chi} = -\frac{1}{2\tilde{E}} (\tilde{\delta P}_1 + \tilde{\delta P}_2) \tag{II.61}$$

where $\tilde{\delta P}_1$ and $\tilde{\delta P}_2$ correspond to the contributions from the soft mode and Goldstone mode, respectively, and are given by Eqs. (II.57)–(II.59). The expressions for $\tilde{\delta P}_1$ and $\tilde{\delta P}_2$ are of course much too involved to permit any perspicuous analytical picture. In Section III.6 we will plot the result of the calculations for some different sets of the input parameters of the equations and compare this with existing experimental data.

At last we shall calculate the dielectric response in the SmA phase. In the equilibrium of the SmA phase the average of the order parameters ξ and \mathbf{P} is zero. This means that the disturbances introduced by the field can be taken to be the order parameters themselves. Expanding the free-energy density given by Eqs. (II.1) and (II.41) to second order in ξ and \mathbf{P} gives

$$\begin{aligned}
 g = g_o + g_E = & \frac{1}{2}a(\xi_1^2 + \xi_2^2) - \Lambda \left(\xi_1 \frac{d\xi_2}{dz} - \xi_2 \frac{d\xi_1}{dz} \right) \\
 & + \frac{1}{2}K_3 \left[\left(\frac{d\xi_1}{dz} \right)^2 + \left(\frac{d\xi_2}{dz} \right)^2 \right] + \frac{1}{2\epsilon} (P_x^2 + P_y^2) \\
 & - \mu \left(P_x \frac{d\xi_1}{dz} + P_y \frac{d\xi_2}{dz} \right) + C(P_x \xi_2 - P_y \xi_1) - EP_x \quad (\text{II.62})
 \end{aligned}$$

The system being in the SmA phase, a homogeneous electric field will couple to $q = 0$ changes of the order parameters. Accordingly we put all spatial derivatives in Eq. (II.62) equal to zero and get

$$g = \frac{1}{2}a(\xi_1^2 + \xi_2^2) + \frac{1}{2\epsilon} (P_x^2 + P_y^2) + C(P_x \xi_2 - P_y \xi_1) - EP_x \quad (\text{II.63})$$

The equilibrium configuration in the presence of the field is then given by demanding $\partial g / \partial \xi_1 = \partial g / \partial \xi_2 = 0$ and $\partial g / \partial P_x = \partial g / \partial P_y = 0$ leading to

$$\begin{aligned}
 a\xi_1 - CP_y &= 0 \\
 a\xi_2 + CP_x &= 0 \\
 (1/\epsilon)P_x + C\xi_2 &= E \\
 (1/\epsilon)P_y + C\xi_1 &= 0
 \end{aligned} \quad (\text{II.64})$$

which has the solution

$$\begin{aligned}\xi_1 &= 0 \\ \xi_2 &= -(C/a)P_x \\ P_x &= \frac{\epsilon a}{a - \epsilon C^2} E \\ P_y &= 0\end{aligned}\quad (II.65)$$

Eqs. (II.39) and (II.65) now give the dielectric susceptibility in the SmA phase

$$\chi_A = \frac{\epsilon a}{a - \epsilon C^2} = \epsilon + \frac{\epsilon^2 C^2}{a - \epsilon C^2} \quad (II.66)$$

By the use of the relation $a = \alpha(T - T_o)$ and the expression of the SmA-SmC* phase transition temperature T_c given by Eq. (II.12), this can be written as

$$\chi_A = \epsilon \frac{\alpha(T - T_c) + \Lambda^2/K_3 + (C + \Lambda\mu/K_3)^2 / \left(\frac{1}{\epsilon} - \mu^2/K_3 \right)}{\alpha(T - T_c) + \Lambda^2/K_3 + (C + \Lambda\mu/K_3)^2 / \left(\frac{1}{\epsilon} - \mu^2/K_3 \right) - \epsilon C^2} \quad (II.67)$$

By using the scaling relation introduced in Section II.4 this can be rewritten into dimensionless form as

$$\tilde{\chi}_A = \frac{\beta^2 - \gamma\tau + \lambda^2}{(1 + \nu^2)(\beta^2 - \gamma\tau + \lambda^2) - (\beta - \lambda\nu)^2} \quad (II.68)$$

The last expression can also be recovered from Eqs. (II.57)–(II.59) and (II.61) by substituting $\bar{\theta}_o = 0$, $\bar{P}_o = 0$ and $\bar{P}_o/\bar{\theta}_o = \beta$ into them. The reason of introducing the last relation is given by Eq. (II.11) which, together with the scaling relations introduced in Section II.4,

implies

$$\lim_{T \rightarrow T_c} \frac{\tilde{P}_o}{\tilde{\theta}_o} = \beta \quad (\text{II.69})$$

II.8 The heat capacity

One important quantity to probe the outcome of the theoretical model is the heat capacity per unit volume C_p of the system. As was discussed in Section II.1 heat capacity data is the motivation^{19,20} to include the c -term in the free-energy density of Eq. (II.1). Once we have established the material parameters of the system we can calculate C_p according to its definition

$$C_p = -T \left(\frac{d^2 g_o}{dT^2} \right)_p \quad (\text{II.70})$$

This relation transforms into dimensionless form by the use of Eqs. (II.16) and (II.17) as

$$\tilde{C}_p = - \left(\frac{T_c}{T^*} - \tau \right) \left(\frac{d^2 \tilde{g}_o}{d\tau^2} \right)_p \quad (\text{II.71})$$

By the use of the operator identity

$$\frac{d}{d\tau} = \frac{\partial}{\partial \tau} + \frac{d\theta}{d\tau} \frac{\partial}{\partial \theta} + \frac{dP}{d\tau} \frac{\partial}{\partial P} \quad (\text{II.72})$$

we can transform the expression (II.71) of \tilde{C}_p into

$$\tilde{C}_p = \left(\frac{T_c}{T^*} - \tau \right) \frac{\left(\frac{\partial^2 \tilde{g}_o}{\partial \tau \partial \theta} \right)^2 \frac{\partial^2 \tilde{g}_o}{\partial \tilde{P}^2}}{\frac{\partial^2 \tilde{g}_o}{\partial \theta^2} \frac{\partial^2 \tilde{g}_o}{\partial \tilde{P}^2} - \left(\frac{\partial^2 \tilde{g}_o}{\partial \theta \partial \tilde{P}} \right)^2} \quad (\text{II.73})$$

where the derivatives which enter Eq. (II.73) can be calculated from Eq. (II.19). The use of Eq. (II.73) instead of Eq. (II.71) allows us to perform the numerical computation of \tilde{C}_p in a more straightforward way.

III. GENERAL BEHAVIOUR OF THE SOLUTIONS OF THE GOVERNING EQUATIONS—COMPARISON WITH EXPERIMENTAL DATA

In this section we will show that the extended Landau expression of the free-energy density introduced by Eq. (II.1) is capable of describing all the features of the ferroelectric SmC* phase in a qualitatively correct way. All the shortcomings of previous models of ferroelectric SmC* liquid crystals which were discussed in the Introduction have thus been removed. We will work within the renormalized, dimensionless model, which was introduced in Section II.4. By comparing the outcome of the calculations with experimental data we will make an estimation of the dimensionless parameters (Eqs. (II.13) and (II.15)) and the scaling factors (Eqs. (II.17)). We then continue by discussing in which way the predictions of our model concerning the temperature dependence of tilt, polarization, pitch, dielectric susceptibility and heat capacity depend on the values of these parameters.

III.1 An estimation of the material parameters of DOBAMBC—general features of the parameters

In Section II we derived the general equations governing the behaviour of ferroelectric SmC* liquid crystals. The model was based on the Landau expansion introduced by Eq. (II.1) and contains altogether eleven material parameters. By the transformation of the equations into dimensionless form, which was performed in Section II.4, we reduced the number of independent parameters determining the temperature dependence of the basic quantities into six (Eqs. (II.13) and (II.15)): γ , β , ρ , λ , δ and ν . In this context we also introduced a number of scaling factors (Eqs. (II.17)). Five of these (T^* , θ^* , P^* , p^* and χ^*) together with the six dimensionless parameters which are enumerated above give the eleven constants, which in our dimensionless model replace the original eleven material parameters. It is easy to check from the definition, that there is a one to one correspondence between the two sets of parameters. As the values of the parameters are obtained by fitting the outcome of the calculations to available experimental data, the determination of the constants is simplified within the dimensionless model as we have reduced the number of free parameters of the model from eleven to six. The scaling factors can then be determined one by one by comparison

with the proper experimental quantity. Still, however, the fitting procedure is quite involved, and in this work we will be satisfied with an estimation of the values of the parameters.

In Figure 5 the crosses represent our measured data of the polarization,⁶ the pitch¹⁰ and the dielectric susceptibility¹⁷ of DOBAMBC. The solid lines represent the outcome of a numerical solution of the governing equations using the parameter values $\gamma = 2.0$, $\beta = -0.17$, $\rho = 0.9$, $\lambda = -0.062$, $\delta = -0.012$ and $\nu = -0.060$. We have chosen the signs of λ , δ and ν in such a way that we are describing a LH(−) type of substance (c.f. Section II.5). The scaling factors, all of which can be determined by also using available data of tilt² and of heat capacity,²⁰ have been taken to be $T^* = 0.92\text{K}$, $P^* = 1.3 \times 10^{-5}\text{C/m}^2$, $p^* = 1.46 \times 10^{-8}\text{m}$, $\chi^* = 2.66 \times 10^{-13}\text{As/Vm}$, $\theta^* = 0.20\text{rad}$ and $C_p^* = 900\text{J/m}^3\text{K}$. In this way six scaling factors have been determined. As only five of these are independent we can use one of the relations (II.18) to check the consistency of the values of the parameters we have chosen. By Eqs. (II.18) we have $C_p^* = P^{*2}/(\chi^*T^*) = 690\text{J/m}^3\text{K}$ which shall be compared with the value of C_p^* which is given above.

In Table II we sum up the values of the parameters given above and also the corresponding values of the original parameters entering the free-energy density. As comparison we give the values of these parameters which also have been obtained by Dumrongrattana and Huang.³⁰ The difference in sign in some of the parameters is due to the fact that in reference 30 the parameters correspond to the RH(+) variant of DOBAMBC.

The parameters which enter our model can be demanded to fulfil some general relations. Thermodynamic stability demands $\gamma > 1$ (Section III.4). A qualitative correct description of the specific heat demands $\rho \sim \gamma$ (Section III.7). There is however no general rule prohibiting ρ to be smaller than unity, and we shall often find it convenient to discuss our model in the limit $\rho = 0$. The known experimental behaviour of the pitch can only be fulfilled as long as $|\beta| < 1$ (Sections II.5 and III.5). The weak chirality of the system together with the experimental behaviour of the pitch furtheron demand $|\lambda|$, $|\nu|$, $|\delta| < |\beta|$ (Section II.5 and III.5). The signs of the four last coefficients must be chosen to be one of the four combinations from group I of Figure 3, in order to give a correct behaviour of the pitch. We thus summarize that all sets of parameters which shall be capable of describing the ferroelectric SmC* phase must fulfil: $\gamma > 1$, $\rho \sim \gamma$, $|\beta| < 1$, and $|\lambda|$, $|\nu|$, $|\delta| < |\beta|$.

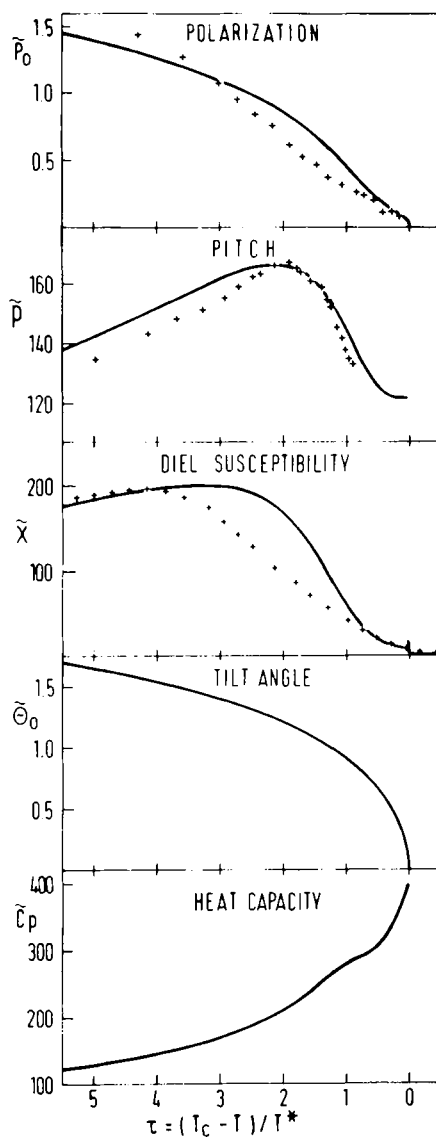


FIGURE 5 Calculated \tilde{P}_0 , \tilde{p} , $\tilde{\chi}$, $\tilde{\theta}_0$ and \tilde{C}_p versus τ . The parameters used are: $\gamma = 2.0$; $\beta = -0.17$; $\rho = 0.90$; $\lambda = -0.062$; $\nu = -0.060$ and $\delta = -0.012$. The crosses represent our experimental values obtained for DOBAMBC.

TABLE II
Estimated values of the material parameters of DOBAMBC. As a comparison to our values we also give those obtained by Huang and Dumrongratana.³⁰

DIMENSIONLESS MODEL												
Parameter	γ	β	ρ	λ	ν	δ	$T^*[\text{K}]$	$\theta^*[\text{rad}]$	$p^*[\text{C}/\text{m}^2]$	$p^*[\text{m}]$	$\chi^*[\text{C}/\text{Vm}]$	$C_p^*[\text{J}/\text{m}^3\text{K}]$
This work	2.0	-0.17	0.90	-0.062	-0.060	-0.012	0.92	0.20	1.3×10^{-5}	1.46×10^{-8}	2.66×10^{-13}	900

ORIGINAL MODEL												
Parameter	$\alpha[\text{N}/\text{m}^2\text{K}]$	$b[\text{N}/\text{m}^2]$	$c[\text{N}/\text{m}^2]$	$\Lambda[\text{N}/\text{m}]$	$K_3[\text{N}]$	$d[\text{N}/\text{m}]$	$\epsilon[\text{C}/\text{Vm}]$	$r[\text{Nm}^6/\text{C}^4]$	$u[\text{V}]$	$c[\text{V}/\text{m}]$	$\Omega[\text{Nm}^2/\text{C}^2]$	
This work	3.5×10^4	8.0×10^5	9.0×10^6	-1.4×10^{-5}	3.4×10^{-12}	-7.0×10^{-5}	2.7×10^{-13}	2.2×10^{22}	-0.21	-4.1×10^7	9.4×10^{13}	
Ref. 30	4.6×10^4	5.2×10^5	9.0×10^6	2.3×10^{-5}	2.5×10^{-12}	2.5×10^{-5}	2.6×10^{-11}	3.8×10^{19}	-0.22	2.8×10^6	5.7×10^{11}	

III.2 A quantitative estimation of the magnitude of the effects due to the unwinding of the helix

In Section II.6 we discussed unwinding effects, deriving expressions relating the governing equations in the cases where the helix is still present in the medium or not. We showed that the structure of the governing equations remains the same in the two cases, however the scaling factors and the parameters which enter the equations will be changed slightly. Having estimated the dimensionless parameters in Section III.1, we now are in a position to evaluate numerically the relations derived in Section II.6. The relations connecting the scaling factors in the two cases are given by Eqs. (II.29). Still we let the index h denote the corresponding symbol when the helix is unwound (the homogeneous case). Using the values of the parameters given by Table I the relative changes of the scaling factors can be expressed as

$$\begin{aligned}\frac{\theta_h^* - \theta^*}{\theta^*} &\approx \frac{1}{2}v^2 \approx 1.8 \times 10^{-3}, & \frac{P_h^* - P^*}{P^*} &\approx \frac{1}{2}v^2 \approx 1.8 \times 10^{-3} \\ \frac{g_h^* - g^*}{g^*} &\approx 2v^2 \approx 7.2 \times 10^{-3} \\ \frac{C_{ph}^* - C_p^*}{C_p^*} &\approx v^2 - \frac{4\lambda\delta}{\gamma} \approx 2.1 \times 10^{-3} \\ \frac{T_h^* - T^*}{T^*} &\approx v^2 + \frac{4\lambda\delta}{\gamma} \approx 5.1 \times 10^{-3}\end{aligned}\quad (\text{III.1})$$

The relation connecting C_{ph}^* and C_p^* can be derived by the use of $C_p^* = g^*/T^*$ which is implicitly given by Eqs. (II.18). The relative changes of the parameters given by Eqs. (II.33) can be expanded as

$$\begin{aligned}\frac{\gamma_h - \gamma}{\gamma} &= \frac{4\lambda\delta}{\gamma} \approx 1.5 \times 10^{-3}, & \frac{\beta_h - \beta}{\beta} &\approx -\frac{\lambda v}{\beta} - v^2 \approx 0.018 \\ \frac{\rho_h - \rho}{\rho} &\approx v^2 + \frac{3\delta^2}{\rho} \approx 4.1 \times 10^{-3}\end{aligned}\quad (\text{III.2})$$

Furtheron Eqs. (II.35) demand

$$\lambda_h = v_h = \delta_h = 0 \quad (\text{III.3})$$

Concerning the reduced temperature, the unwinding not only changes the scaling factor slightly as is seen from the last of Eqs. (III.1) but also shifts the phase transition temperature and we get according to Eqs. (II.23) and (II.36)

$$\begin{aligned} T_c - T_{ch} &= \frac{T^*}{\gamma} \left[\beta^2 + \lambda^2 - \beta^2 \frac{(1 - \lambda\nu/\beta)^2}{1 + \nu^2} \right] \\ &\approx \frac{T^*}{\gamma} \lambda^2 \approx 1.8 \times 10^{-3} K \end{aligned} \quad (\text{III.4})$$

showing that the shift of T_c is negligible.

We thus conclude that the relative changes of the scaling factors of the physically measurable quantities as temperature, tilt, polarization and heat capacity are affected less than half a percent by the unwinding of the helix. Concerning the equations governing the tilt and polarization we see by comparing Eqs. (II.20) and (II.21) with Eqs. (II.37) and (II.38) that the effects of the unwinding of the helix can be expected to induce changes in these quantities which are of the order of one percent. The conclusion we want to draw by these numerical estimations is that the effects of unwinding of the helix are so small, smaller than the experimental uncertainty, that we do not need to keep track whether the experimental data we examine are obtained from an unwound sample or not.

III.3 Analytical solution of the polarization equation—the possibility of sign reversal of the polarization

The temperature dependence of the tilt and the polarization are given by Eqs. (II.20) and (II.21)

$$(\beta^2 - \gamma\tau)\tilde{\theta}_o + \gamma\tilde{\theta}_o^3 + \rho\tilde{\theta}_o^5 - \tilde{\theta}_o\tilde{P}_o^2 - (\beta + 3\nu\delta\tilde{\theta}_o^2)\tilde{P}_o = 0 \quad (\text{II.20})$$

$$\tilde{P}_o^3 + (1 - \tilde{\theta}_o^2)\tilde{P}_o - (\beta + \nu\delta\tilde{\theta}_o^2)\tilde{\theta}_o = 0 \quad (\text{II.21})$$

To achieve the correct solution of these equations we proceed as follows. Using $\tilde{\theta}_o$ as input parameter Eq. (II.21) provides a cubic equation in \tilde{P}_o . This equation has one or three real roots. In the case when the equation has one root the problem is straightforward. We just substitute $\tilde{\theta}_o$ and \tilde{P}_o into Eq. (II.20) and calculate directly the corresponding temperature τ . In this way we obtain implicitly $\tilde{\theta}_o(\tau)$ and $\tilde{P}_o(\tau)$. In the case when the equation has three roots, which we denote \tilde{P}_o^+ , \tilde{P}_o^- and \tilde{P}_o^0 , the situation gets more involved. Each of

these solutions now has to be substituted into Eq. (II.20) together with the starting value of $\tilde{\theta}_o$. In this way we calculate three slightly different values of the corresponding temperature which we denote τ^+ , τ^- and τ^o . One solution (τ^o , \tilde{P}_o^o , $\tilde{\theta}_o$) can be showed to correspond to a local maximum of the free-energy density (Eq. (II.19)) while the solutions (τ^+ , \tilde{P}_o^+ , $\tilde{\theta}_o$) and (τ^- , \tilde{P}_o^- , $\tilde{\theta}_o$) both correspond to local minima. We thus have to choose the solution for which the free-energy density is minimized. The problem which now arises is that nature does not solve the problem in the same way as the computer. In the real system temperature is the input parameter, and we shall not compare the free-energy density of the solutions (τ^+ , \tilde{P}_o^+ , $\tilde{\theta}_o$) and (τ^- , \tilde{P}_o^- , $\tilde{\theta}_o$) but the free-energy density of the solutions where $\tau^+ = \tau^- = \tau$, which corresponds to slightly shifted values of the input parameter $\tilde{\theta}_o$. These solutions are denoted (τ , \tilde{P}_o^+ , $\tilde{\theta}_o^+$) and (τ , \tilde{P}_o^- , $\tilde{\theta}_o^-$), respectively.

In order to write down the solution of Eq. (II.21) we first introduce the parameter x according to

$$x = \frac{\sqrt{27}}{2} \frac{(\beta + \nu \delta \tilde{\theta}_o^2) \tilde{\theta}_o}{|1 - \tilde{\theta}_o^2|^{3/2}} \quad (\text{III.5})$$

Depending on the values of x and $\tilde{\theta}_o$ we get three regimes of the solution.

Regime 1: $\tilde{\theta}_o < 1$

One real solution

$$\tilde{P}_o = \frac{2}{\sqrt{3}} (1 - \tilde{\theta}_o^2)^{1/2} \sinh \left(\frac{1}{3} \sinh^{-1} x \right) \quad (\text{III.6})$$

Regime 2: $\tilde{\theta}_o > 1$; $|x| > 1$

One real solution

$$\tilde{P}_o = \frac{x}{|x|} \frac{2}{\sqrt{3}} (\tilde{\theta}_o^2 - 1)^{1/2} \cosh \left(\frac{1}{3} \cosh^{-1} |x| \right) \quad (\text{III.7})$$

Regime 3: $\tilde{\theta}_o > 1$; $|x| < 1$

Three real solutions—one of which corresponds to a maximum of g_o and is not considered here

$$\tilde{P}_o = \tilde{P}_o^+ = \frac{2}{\sqrt{3}} (\tilde{\theta}_o^2 - 1)^{1/2} \cos \left(\frac{1}{3} \cos^{-1} x \right) \quad (x_c < x < 1) \quad (\text{III.8a})$$

$$\tilde{P}_o = \tilde{P}_o^- = -\frac{2}{\sqrt{3}} (\tilde{\theta}_o^2 - 1)^{1/2} \cos \left(\frac{1}{3} \cos^{-1}(-x) \right) \quad (-1 < x < x_c) \quad (\text{III.8b})$$

In the third regime we now have to choose the one of the solutions $(\tau, \tilde{P}_o^+, \tilde{\theta}_o^+)$ and $(\tau, \tilde{P}_o^-, \tilde{\theta}_o^-)$ which minimizes the free-energy density of Eq. (II.19). We must however observe, that we shall compare the two solutions which correspond to the same value of τ , i.e. the expressions of Eqs. (III.8a) and (III.8b) with slightly shifted values of $\tilde{\theta}_o$. This comparison has to be performed numerically. It turns out that \tilde{P}_o^+ is the stable solution when $x_c < x < 1$ while \tilde{P}_o^- is the stable one when $-1 < x < x_c$. The tilt angle at the transition from the \tilde{P}_o^+ to the \tilde{P}_o^- solution is denoted by $\tilde{\theta}_c$. We have found by careful numerical studies that x_c is approximately zero. Putting $x_c = 0$, admits a prediction of θ_c with an accuracy which, expressed in physical units, is of the order of 10^{-3} degrees. This is well within the experimental uncertainty. Eq. (III.5) thus gives, putting $x_c = 0$, the following "almost exact" determination of $\tilde{\theta}_c$

$$\tilde{\theta}_c^2 = -\frac{\beta}{\nu\delta}, \quad \theta_c^2 = -\frac{\tilde{C}K_3}{d\mu} \quad (\text{III.9})$$

where the relation is given both in dimensionless and physical units. This relation also covers the possibility of change of sign of \tilde{P}_o within regime 1, where it is an exact one.

The solution of the polarization equation is schematically illustrated in Figure 6 in the case when $\tilde{\theta}_c^2 > 1$. The transition from the \tilde{P}_o^+ to the \tilde{P}_o^- solution, which in reality will be rounded off by thermal fluctuations, would correspond to the transition from a (+) to a (−) substance according to the nomenclature by Clark and Lagerwall.²⁵ Such a transition has recently been reported by Goodby *et al.*³² to occur for some compounds. Calculating θ_c by substituting the two sets of parameters of DOBAMBC, which are given by Table II, into Eqs. (III.9) gives $\theta_c \approx 180^\circ$ using the parameters chosen in this work and $\theta_c \approx 34^\circ$ using the parameters given by Huang and Dumrongrattana.³⁰ In the first case $\tilde{\theta}_c$ is nonphysical but also in the second case the angle is without experimental range as the transition to the SmI* phase occurs at a smaller angle. This means that the problem of the change of stability between the \tilde{P}_o^+ and \tilde{P}_o^- solution in Eqs. (III.8) for most compounds seems to be only of academical interest and thus only the \tilde{P}_o^+ solution has to be considered within the range

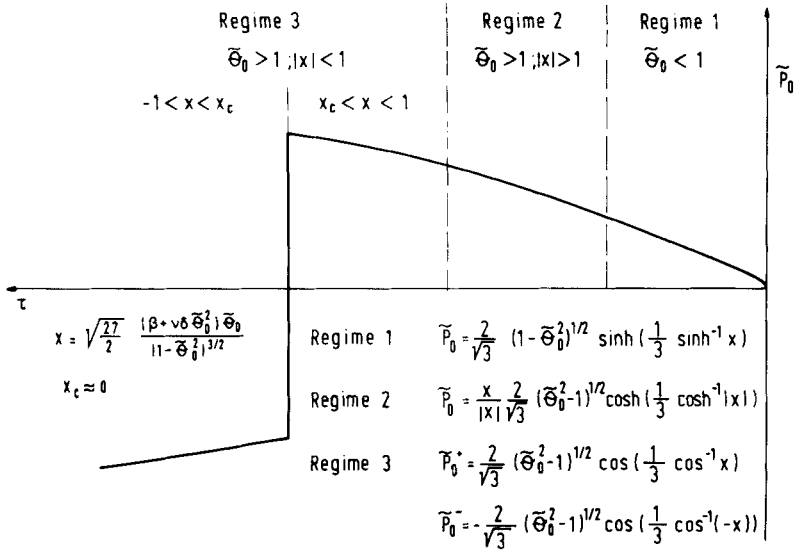


FIGURE 6 The three regimes of the solution of the polarization equation (II.21).

of the SmC* phase. Still however we do not need to change the parameters very much in order to decrease $\tilde{\theta}_c$ into an experimentally observable value, and we mention once more that compounds exhibiting a change of sign in polarization have recently been reported.³² The possibility of such a transition is thus predicted by our model and the value of the tilt angle at the transition is given by Eqs. (III.9).

III.4 General behaviour of the solutions of the equations governing tilt and polarization

In this section we will study the solution of the tilt and the polarization equations (II.20) and (II.21) in detail. We still only consider the case $|\beta| < 1$ as was discussed in Section II.5. Being interested in the system mainly close to T_c , we will not take into account the possibility of the transition from the \tilde{P}_0^+ to the \tilde{P}_0^- solution which was discussed in connection to Eqs. (III.8) in the previous section, but we will assume that the material parameters adopt such values that the parameter x introduced by Eq. (III.5) always satisfies $x > x_c$. With our choice of parameters, which is given by Table II, this is certainly fulfilled. By also observing from Figure 5 that $\tilde{\theta}_0$ in this case is of the order of unity, we can neglect the terms containing $\nu\delta$ in the equations ($|\nu\delta| \approx 7 \times 10^{-4} \ll |\beta| \approx 0.17$). This means that in this

case only three parameters rule the behaviour of tilt and polarization and Eqs. (II.20) and (II.21) simplify into

$$(\beta^2 - \gamma\tau)\tilde{\theta}_o + \gamma\tilde{\theta}_o^3 + \rho\tilde{\theta}_o^5 - \tilde{\theta}_o\tilde{P}_o^2 - \beta\tilde{P}_o = 0 \quad (\text{III.10})$$

$$\tilde{P}_o^3 + (1 - \tilde{\theta}_o^2)\tilde{P}_o - \beta\tilde{\theta}_o = 0 \quad (\text{III.11})$$

The approximations leading to these equations are valid not only close to T_c but, for most compounds, also in the entire SmC^* phase. The ρ -term in the free-energy density was introduced in order to describe^{19,20} the bent shape of the heat capacity close to T_c . Concerning the solution of Eqs. (III.10) and (III.11), reasonable values of ρ (i.e. $\rho \lesssim \gamma$) do not add any qualitatively new features, but merely introduce saturation effects for large tilt angles, a fact which is clearly demonstrated in Figure 7 where we have plotted polarization and tilt versus temperature for $\gamma = 2.0$, $\beta = 0.20$ and varying ρ from zero to 5.0. This means that the qualitative behaviour of tilt and polarization, especially close to T_c , is most conveniently discussed within the approximation $\rho = 0$. In this way we have reduced the number of free parameters entering the equations to two, γ and β . Even in this simple model it is hard to derive analytical solutions of $\tilde{\theta}_o(\tau)$ and $\tilde{P}_o(\tau)$. In the limits $\tau \rightarrow 0$ and $\tau \rightarrow \infty$ we however can give the following approximate solutions of the equations

$\tau \rightarrow 0$ (approximation: $\rho = \nu\delta = 0$)

$$\begin{aligned} \tilde{\theta}_o^2 &= \frac{\tau}{1 - 2\frac{\beta^2}{\gamma} + \frac{\beta^4}{\gamma}} \\ \tilde{P}_o &= \beta\tilde{\theta}_o + (\beta - \beta^3)\tilde{\theta}_o^3 \end{aligned} \quad (\text{III.12})$$

$\tau \rightarrow \infty$ (approximation: $\rho = \nu\delta = 0$)

$$\begin{aligned} \tilde{\theta}_o^2 &= \frac{\gamma\tau}{\gamma - 1} \\ \tilde{P}_o &= \tilde{\theta}_o \end{aligned} \quad (\text{III.13})$$

The first of Eqs. (III.13) implies $\gamma > 1$ in order to certify the thermodynamical stability of the system.

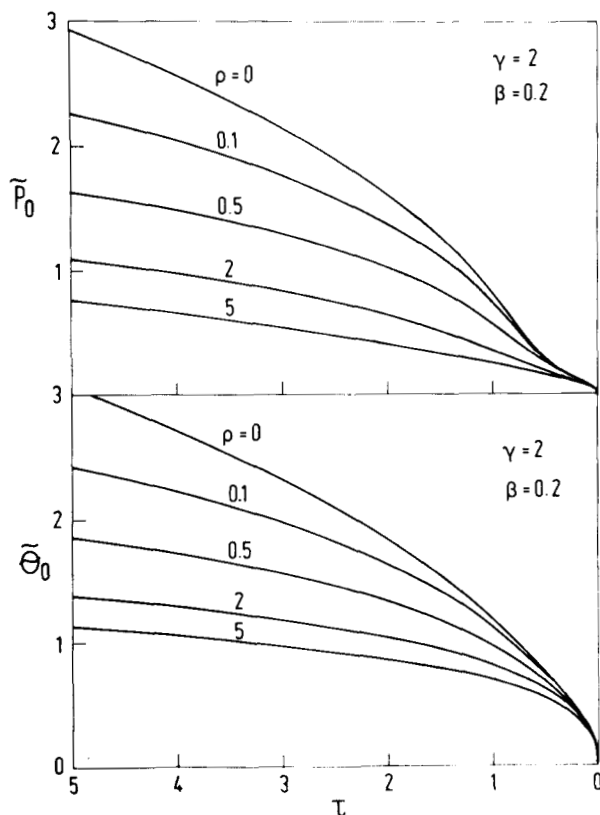


FIGURE 7 Influence of the parameter ρ on the temperature dependence of polarization and tilt.

From Eqs. (III.12) and (III.13) we expect different square-root behaviours of tilt and polarization versus temperature in the limits $\tau \rightarrow 0$ and $\tau \rightarrow \infty$. This behaviour manifests itself, for certain combinations of the parameters, in such a way that the polarization curve is S-shaped. Also the tilt exhibits in some cases a small anomaly in the same region. In Figures 8 and 9 we show two sequences of curves, calculated by keeping one of the parameters γ and β fixed, while the other one is varied within a suitable interval in the case $\rho = 0$. The S-shape has also been found experimentally in the polarization of some compounds.^{6,8,9} In contrast to the S-shaped polarization which we have found experimentally in DOBAMBC⁶ (c.f. Figure 5) other authors have presented polarization measurements of DOBAMBC⁷ which do not exhibit an S-shape. In order to investigate which pa-



Downloaded by [Tomsk State University of Control Systems and Radio] at 12:44 19 February 2013

Downloaded by [Tomsk State University of Control Systems and Radio] at 12:44 19 February 2013

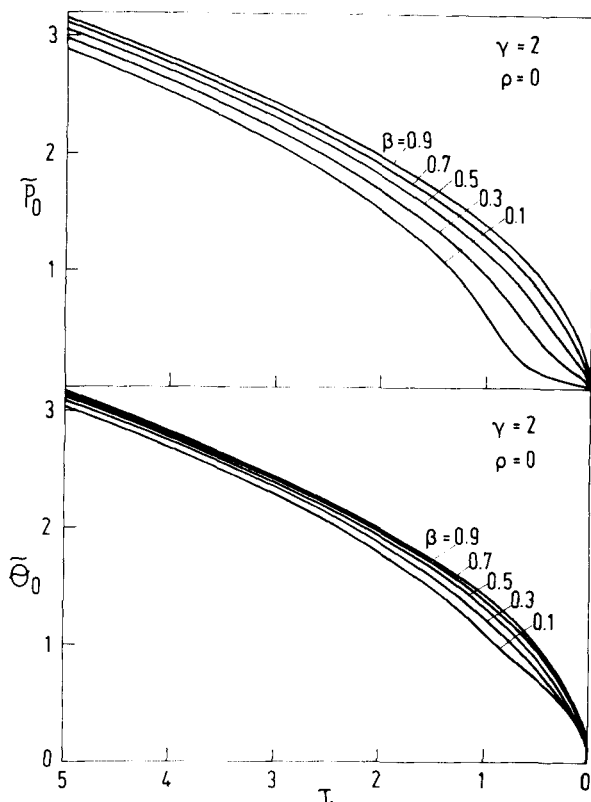


FIGURE 9 Influence of the parameter β on the temperature dependence of polarization and tilt.

corresponds to the limiting case. As our criterion determining the S-shape is a purely mathematical one, it is however hard to recognize the S-shaped feature of the curves close to β_c by the eye. Choosing the value $\gamma = 2.0$ we further on investigate in which part of the $\zeta\beta$ plane S-shaped polarization curves are produced. We notice that introducing ρ into the model suppresses the tendency of S-shape, but still the limiting curve $\beta_c(\rho)$ seems to saturate. We calculated $\beta_c(\rho = 8) \approx 0.18$ and $\beta_c(\rho = 14) \approx 0.17$. In the case $\gamma = 2$, the value $\rho = 14$ must indeed be considered to be a very large one as will be clarified in Section III.7. The conclusion which one can draw from this investigation, is that as well S-shaped as non S-shaped polarization curves are admitted by reasonable values of the parameters.

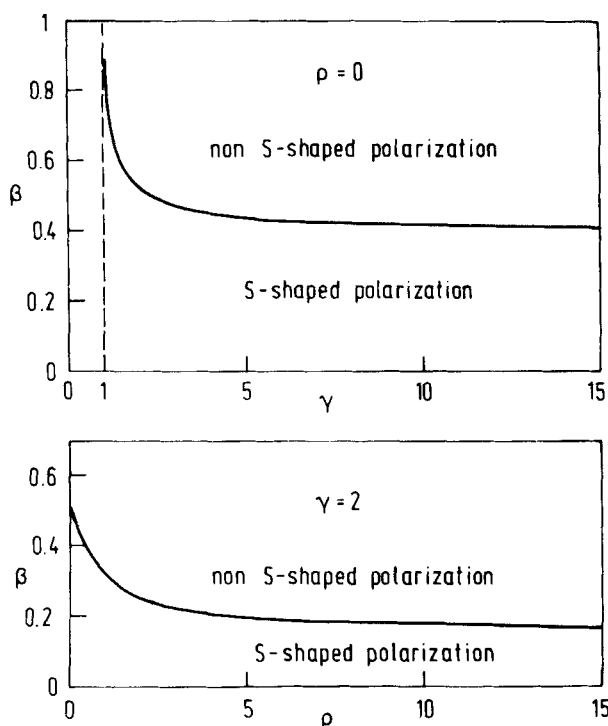


FIGURE 10 Influence of the parameters γ , β and ρ on the shape of the curve of polarization versus temperature.

In connection to the discussion of S-shaped polarization curves we also discuss the behaviour of the ratio between polarization and tilt. Again the experimental behaviour of $\tilde{P}_o/\tilde{\theta}_o$ versus τ has been reported^{7,9} to exhibit an anomaly close to T_c , i.e. in the same region as the “knee” in the polarization curves have been found. From Eqs. (III.12) and (III.13) we can immediately calculate $\tilde{P}_o/\tilde{\theta}_o$ in the limits of large and small τ (Still within approximation $\rho = 0$; $|\beta| \gg |\nu\delta|\tilde{\theta}_o^2$).

$$\lim_{\tau \rightarrow 0} \frac{\tilde{P}_o}{\tilde{\theta}_o} = \beta, \quad \lim_{\tau \rightarrow \infty} \frac{\tilde{P}_o}{\tilde{\theta}_o} = 1 \quad (\text{III.14})$$

We thus note a transition region, where the ratio $\tilde{P}_o/\tilde{\theta}_o$ changes from the value $\tilde{P}_o/\tilde{\theta}_o = \beta$, ($|\beta| < 1$), close to T_c to the value of unity far

from T_c . By dividing the polarization equation (II.21) by θ_o^3 we can rewrite it as

$$\left(\frac{\tilde{P}_o}{\tilde{\theta}_o}\right)^3 + \left(\frac{1}{\tilde{\theta}_o^2} - 1\right) \frac{\tilde{P}_o}{\tilde{\theta}_o} - \frac{\beta}{\tilde{\theta}_o^2} - \nu\delta = 0 \quad (\text{III.15})$$

where we have retained the $\nu\delta$ -term in Eq. (III.15) at this stage for completeness. Recalling the fundamental assumption in the beginning of this section ($|\nu\delta|\tilde{\theta}_o^2 \ll |\beta| < 1$) Eq. (III.15) shows that the ratio $\tilde{P}_o/\tilde{\theta}_o$ as function of $\tilde{\theta}_o^2$ depends on one parameter only, namely β . In Figure 11 we have plotted a sequence of such curves varying β from 0.1 to 0.9. We notice, that also these curves exhibit a change of sign of their second derivative (S-shaped behaviour) when β is small enough.

We thus can conclude that even if the original equations determining tilt and polarization are quite complicated, depending on a vast number of parameters, and not permitting any straightforward analytical solutions, we can get a good qualitative understanding of

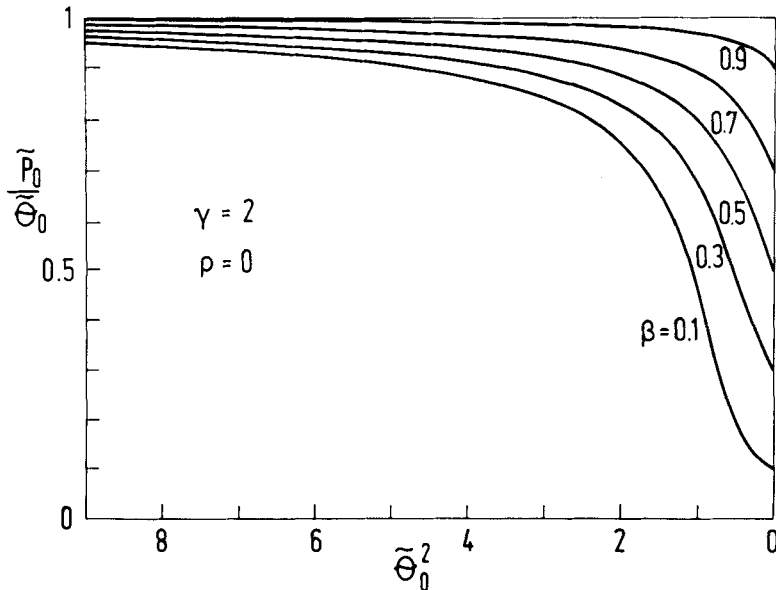


FIGURE 11 The ratio polarization/tilt as a function of tilt-squared. The only parameter which influences the behaviour of the curves (in the limit $|\beta| \gg |\nu\delta|$) is β as is readily seen from Eq. (III.15).

the behaviour of their solutions basically by the use of one parameter, namely β . Expressing β in the original parameters entering the free-energy density of Eq. (II.1) we get

$$\beta = \frac{\tilde{\epsilon} \tilde{C} \eta^{1/2}}{\Omega^{1/2}} \quad (\text{III.16})$$

As the anomalous behaviour of the polarization is showed to be connected to keeping z small we conclude that the anomaly is related to the influence of the biquadratic coupling (the Ω -term) between tilt and polarization in the free-energy density. Thus a weak biquadratic coupling between tilt and polarization gives polarization curves of the “classical” non S-shaped type, while a strong biquadratic coupling is the driving force of the more complicated behaviour which manifests itself by the anomalies in the polarization and polarization/tilt curves close to T_c .

III.5 Behaviour of the pitch

The wave vector of the pitch is given by Eq. (II.22)

$$\tilde{q} = \lambda + \nu \frac{\tilde{P}_o}{\tilde{\theta}_o} + \delta \tilde{\theta}_o^2 \quad (\text{II.22})$$

As $\tilde{P}_o/\tilde{\theta}_o$ is shown by Eq. (III.15) to be a function of $\tilde{\theta}_o^2$ we conclude that the same is also true concerning the pitch. In order to simplify the discussion in this section we discuss the case of a RH(+) type of substance. This means that the signs of the quantities entering Eq. (II.22) are as follows (c.f. Figure 3): $\lambda > 0$, $\nu < 0$, $\tilde{P}_o/\tilde{\theta}_o > 0$ and $\delta > 0$. More conveniently we then write the expression of q as

$$\tilde{q} = \lambda - |\nu| \frac{\tilde{P}_o}{\tilde{\theta}_o} + \delta \tilde{\theta}_o^2 \quad (\text{III.17})$$

The general behaviour of the pitch as function of temperature is shown by our experimental data in Figure 5. At low temperatures it slowly increases with increasing temperature, reaching a maximum at approximately 1K below T_c and then sharply decreases to a finite value at T_c . Concerning \tilde{q} ($\tilde{q} = 2\pi/\tilde{p}$) as function of $\tilde{\theta}_o$ the behaviour is thus such that \tilde{q} starts from a finite value at T_c , decreases towards a minimum approximately 1K below T_c and then slowly increases with increasing value of $\tilde{\theta}_o$ (decreasing absolute temperatures).

From Eqs. (II.21) and (III.17) we calculate \tilde{q} to first order in $\tilde{\theta}_o^2$ close to T_c .

$$\tilde{q}(\tau \rightarrow 0) \simeq \lambda - |\nu|\beta - [|\nu|(\beta - \beta^3 - |\nu|\delta) - \delta]\tilde{\theta}_o^2 \quad (\text{III.18})$$

We note from Eq. (III.18) that the slope of $\tilde{q}(\tau)$ close to T_c is determined by the sign of the factor $|\nu|(\beta - \beta^3) - \delta$. In the limit which we are working this factor is always positive (for positive β) and smaller than unity ($|\beta| < 1$; $|\nu|, |\delta| < |\beta|$). Increasing $\tilde{\theta}_o$ we thus at first stage can neglect the term $|\delta|\tilde{\theta}_o^2$ in Eq. (III.17). We know from Figure 11 that $\tilde{P}_o/\tilde{\theta}_o$ is an increasing function of $\tilde{\theta}_o$ implying that the second term in Eq. (III.17) will be responsible of the decrease in \tilde{q} as τ is increased. As $\tilde{\theta}_o$ is increased further, the ratio $\tilde{P}_o/\tilde{\theta}_o$ rapidly saturates towards unity and the term $\delta\tilde{\theta}_o^2$ will then be responsible of increasing \tilde{q} , which thus, somewhere in the region of the “knee” of the $\tilde{P}_o/\tilde{\theta}_o$ curve, must exhibit a minimum. In the limit of large $\tilde{\theta}_o$, the change of the pitch with temperature is controlled by the $\delta\tilde{\theta}_o^2$ -term and we can write

$$\lim_{\tau \rightarrow \infty} \frac{d\tilde{q}}{d\tilde{\theta}_o^2} = \delta \quad (\text{III.19})$$

a relation which can be used to experimentally determine the parameter δ .

From the discussion above we conclude that the maximum of the pitch is connected to the anomaly of $\tilde{P}_o/\tilde{\theta}_o$ or phrased otherwise, to the anomaly of \tilde{P}_o . A $\tilde{P}_o/\tilde{\theta}_o$ curve which is almost constant would never be capable of producing a minimum of \tilde{q} as given by Eq. (III.17). This is another argument of the importance of the biquadratic coupling (the Ω -term) between tilt and polarization in the free-energy density of Eq. (II.1). In Figure 12 we show the outcome of a calculation of the pitch and the polarization/tilt for some different values of the parameters. This figure clearly demonstrates how the maximum of the pitch is related to the form of the $\tilde{P}_o/\tilde{\theta}_o$ curve.

Finally we point out that a theory where the biquadratic coupling between tilt and polarization is neglected (i.e. with $\Omega = 0$) predicts³³ a temperature independent \tilde{q} , a temperature independent $\tilde{P}_o/\tilde{\theta}_o$ and a pure square-root behaviour of as well $\tilde{\theta}_o$ and \tilde{P}_o . This once more emphasizes the importance of the biquadratic coupling between tilt and polarization in the free-energy density of the ferroelectric SmC* phase.

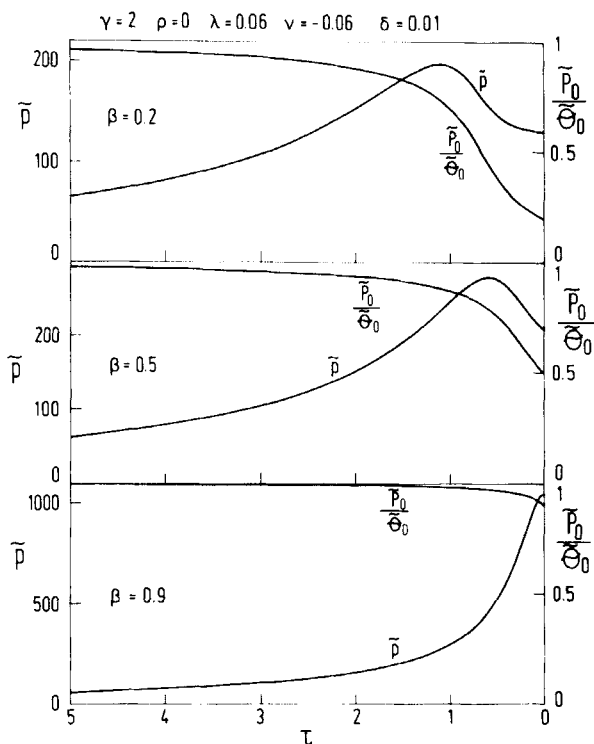


FIGURE 12 Demonstration of the connection between the maximum of the pitch and the “knee” in the polarization/tilt curve.

III.6 The static dielectric susceptibility

The general experimental behaviour of the static dielectric susceptibility $\tilde{\chi}$ of the ferroelectric SmC^* phase is shown in Figure 5. As is discussed in Section II.7, $\tilde{\chi}$ can be divided into two parts; one which is due to the amplitude changes (soft mode) and one which is due to the phase changes (Goldstone mode) of the order parameters. The expression of $\tilde{\chi}$ within our model is given by Eqs. (II.57)–(II.59) and (II.61). Due to a small amplitude—phase coupling, the division of $\tilde{\chi}$ into the soft mode and the Goldstone mode is however not clear-cut. In connection to Eqs. (II.43) we simply defined the soft mode and the Goldstone mode to the parts of $\tilde{\chi}$ which are proportional to the amplitude changes $\delta\tilde{P}_1$ and to the phase changes $\delta\tilde{P}_2$ of the polarization, respectively. Generally an amplitude change of the polarization mostly corresponds to an amplitude change of tilt $\delta\tilde{\theta}_1$,

but it also includes a small phase contribution of the tilt $\tilde{\delta\theta}_2$. We thus can write

$$\tilde{\delta P} = \tilde{\delta P}_I(\tilde{\delta\theta}_1, \tilde{\delta\theta}_2) + \tilde{\delta P}_{II}(\tilde{\delta\theta}_1, \tilde{\delta\theta}_2) \quad (\text{III.20})$$

where the $\tilde{\delta\theta}_1$ dependence is the dominant part of $\tilde{\delta P}_I$ while the $\tilde{\delta\theta}_2$ dependence is the dominant part of $\tilde{\delta P}_{II}$. We now instead divide the total induced polarization in a slightly different way

$$\tilde{\delta P} = \tilde{\delta P}_I(\tilde{\delta\theta}_1) + \tilde{\delta P}_{II}(\tilde{\delta\theta}_2) \quad (\text{III.21})$$

where $\tilde{\delta P}_I$ is the part of the induced polarization which is dependent of $\tilde{\delta\theta}_1$ and $\tilde{\delta P}_{II}$ in the part which is dependent of $\tilde{\delta\theta}_2$. The two parts $\tilde{\delta P}_I$ and $\tilde{\delta P}_{II}$ will thus contain contributions from both $\tilde{\delta P}_1$ and $\tilde{\delta P}_2$ and we can write

$$\begin{aligned} \tilde{\delta P}_I &= a_{11} \tilde{\delta P}_1 + a_{12} \tilde{\delta P}_2 \\ \tilde{\delta P}_{II} &= a_{21} \tilde{\delta P}_1 + a_{22} \tilde{\delta P}_2 \end{aligned} \quad (\text{III.22})$$

In the case of zero amplitude-phase coupling we simply have $a_{11} = a_{22} = 1$ and $a_{12} = a_{21} = 0$. By calculating the deviation of a_{ij} from these values we thus get an estimation of the strength of the amplitude-phase coupling. Eqs. (III.20)–(III.22) imply the following relation

$$a_{11} + a_{21} = a_{12} + a_{22} = 1 \quad (\text{III.23})$$

From Eqs. (II.56) we can derive the following pair of equations

$$\begin{aligned} (\tilde{b}_3\tilde{b}_5 - \tilde{b}_2\tilde{b}_4) \tilde{\delta P}_I + (\tilde{b}_4\tilde{b}_5 - \tilde{b}_2\tilde{b}_6) \tilde{\delta P}_2 &= (\tilde{b}_2^2 - \tilde{b}_1\tilde{b}_5) \tilde{\delta\theta}_1 \\ (\tilde{b}_2\tilde{b}_3 - \tilde{b}_1\tilde{b}_4) \tilde{\delta P}_I + (\tilde{b}_2\tilde{b}_4 - \tilde{b}_1\tilde{b}_6) \tilde{\delta P}_2 &= (\tilde{b}_1\tilde{b}_5 - \tilde{b}_2^2) \tilde{\delta\theta}_2 \end{aligned} \quad (\text{III.24})$$

where the coefficients \tilde{b}_i are defined by Eqs. (II.57). Eqs. (III.24) express simply that some linear combination of $\tilde{\delta P}_I$ and $\tilde{\delta P}_2$ is proportional to $\tilde{\delta\theta}_1$ while another linear combination is proportional to

$\delta\tilde{\theta}_2$. These two linear combinations are, after proper normalization, the two quantities $\delta\tilde{P}_I$ and $\delta\tilde{P}_{II}$ which we are looking for. Eqs. (III.24) together with the conditions (III.23) can now be used to determine the coefficients a_{ij} which define $\delta\tilde{P}_I$ and $\delta\tilde{P}_{II}$ by Eqs. (III.22)

$$\begin{aligned}
 a_{11} &= \frac{(\bar{b}_2\bar{b}_4 - \bar{b}_1\bar{b}_6 - \bar{b}_2\bar{b}_3 + \bar{b}_1\bar{b}_4)(\bar{b}_3\bar{b}_5 - \bar{b}_2\bar{b}_4)}{(\bar{b}_1\bar{b}_5 - \bar{b}_2^2)(\bar{b}_4^2 - \bar{b}_3\bar{b}_6)} \\
 a_{12} &= \frac{(\bar{b}_2\bar{b}_4 - \bar{b}_1\bar{b}_6 - \bar{b}_2\bar{b}_3 + \bar{b}_1\bar{b}_4)(\bar{b}_4\bar{b}_5 - \bar{b}_2\bar{b}_6)}{(\bar{b}_1\bar{b}_5 - \bar{b}_2^2)(\bar{b}_4^2 - \bar{b}_3\bar{b}_6)} \\
 a_{21} &= \frac{(\bar{b}_2\bar{b}_6 + \bar{b}_3\bar{b}_5 - \bar{b}_4\bar{b}_5 - \bar{b}_2\bar{b}_4)(\bar{b}_2\bar{b}_3 - \bar{b}_1\bar{b}_4)}{(\bar{b}_1\bar{b}_5 - \bar{b}_2^2)(\bar{b}_4^2 - \bar{b}_3\bar{b}_6)} \\
 a_{22} &= \frac{(\bar{b}_2\bar{b}_6 + \bar{b}_3\bar{b}_5 - \bar{b}_4\bar{b}_5 - \bar{b}_2\bar{b}_4)(\bar{b}_2\bar{b}_4 - \bar{b}_1\bar{b}_6)}{(\bar{b}_1\bar{b}_5 - \bar{b}_2^2)(\bar{b}_4^2 - \bar{b}_3\bar{b}_6)} \quad (III.25)
 \end{aligned}$$

The magnitude of the nondiagonal coupling coefficients a_{12} and a_{21} is a measure of the amplitude-phase coupling. In Figure 13 we have plotted these coefficients as function of temperature by using our set

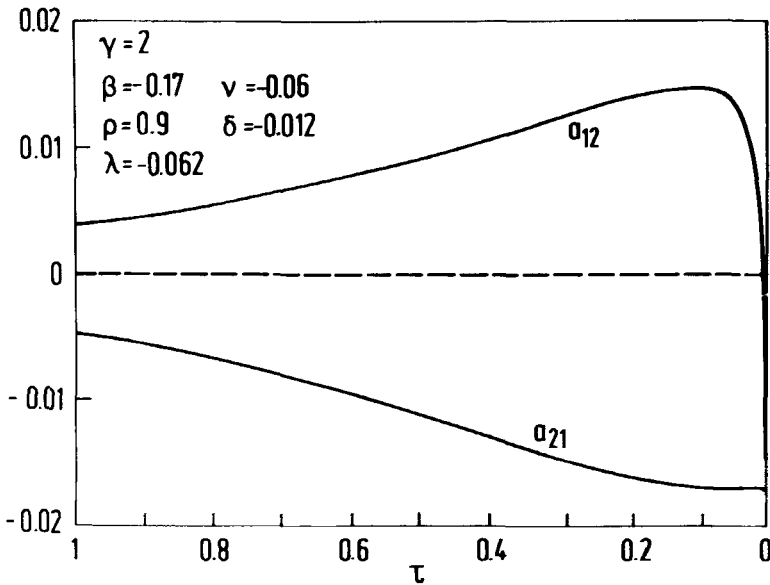


FIGURE 13 Demonstration of the weakness of the amplitude-phase coupling of the fluctuations of the order parameters.

of parameters which is given by Table II. As is seen they are well below 0.01 for all temperatures except a few tenths of degrees below T_c where they increase slightly, however never exceeding a value of 0.02. This means that the amplitude-phase coupling is so weak that, within the experimental error, the definition of the soft mode and the Goldstone mode by the use of $\delta\tilde{P}_1$ and $\delta\tilde{P}_2$ or $\delta\tilde{P}_1$ and $\delta\tilde{P}_{11}$ is immaterial. To make a rigorous separation of the dielectric susceptibility one has to analyse the dynamical equations of the system and determine the two eigenmodes, one of which is mostly phase mode while the other one is mostly amplitude mode. Still however, due to the weak coupling, this more rigorous analysis would add nothing new in the case of the static susceptibility. From the definition of \tilde{b}_i (Eq. (II.57)) we see that the coefficients \tilde{b}_2 and \tilde{b}_4 only contain terms which are proportional to the "small" parameters λ , ν and δ , while all the other \tilde{b}_i contain contributions which are of the order of unity. From the algebraic expressions of a_{ij} given by Eqs. (III.25) we conclude that in the limit $\tilde{b}_2 = \tilde{b}_4 = 0$ we get $a_{11} = a_{22} = 1$ and $a_{12} = a_{21} = 0$. Thus, as soon as the relation $\tilde{b}_2, \tilde{b}_4 \ll \tilde{b}_1, \tilde{b}_3, \tilde{b}_5, \tilde{b}_6, \tilde{b}_7, \tilde{b}_8$ holds, a_{12} and a_{21} will be small, confirming that the weakness of the amplitude-phase coupling is a general property of the system.

In Figure 14 we have plotted the dielectric susceptibility calculated by the use of our set of parameters given by Table II. We also show the separation of χ into the soft mode and the Goldstone mode according to Eq. (II.43). The behaviour shown in Figure 14 reflects the general behaviour of the result of a calculation of χ according to our model. Apart from the broad maximum which is located a few degrees below T_c , the calculations also indicate the existence of a small peak of χ at T_c . In order to verify this experimentally, high resolution temperature measurements are needed to be performed close to T_c . However, in the dielectric measurements by Yoshino et al.,¹² there is an indication of this peak to exist in the dielectric susceptibility of DOBAMBC.

The soft mode χ_1 contributes in both the SmC* and the SmA phase exhibiting a cusp-like peak at T_c , still however being finite. When $|\tau|$ is increased from zero, the contribution from χ_1 is rapidly suppressed to the limiting values zero in the SmC* phase and ϵ in the SmA phase. The absence of a critical divergence at T_c , which is a general feature of the model, is due to the fact that at T_c the SmA phase becomes unstable with respect to helicoidal fluctuations with wave vector $2\pi/p(T_c)$, while in dielectric measurements a homogeneous external field couples to $q = 0$ fluctuations above T_c and $q = 0$ and $q = 4\pi/p$

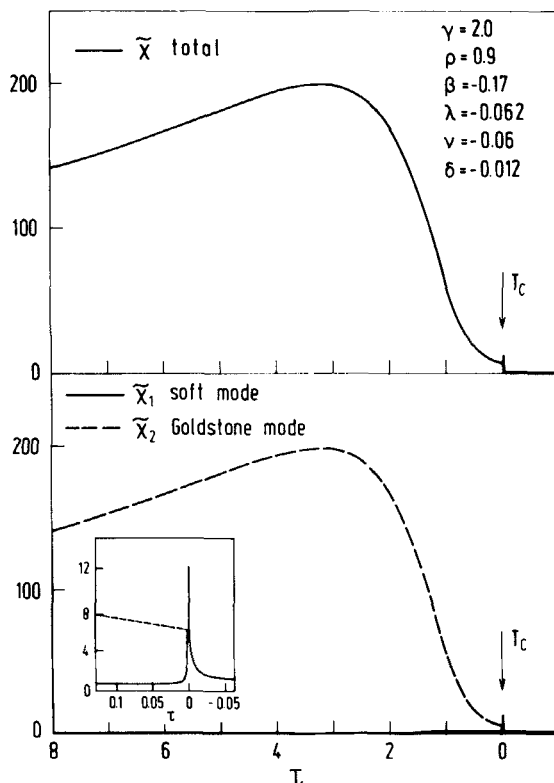


FIGURE 14 Calculation of the dielectric susceptibility according to our model (upper part). In the lower part is shown the division of $\tilde{\chi}$ into the soft mode ($\tilde{\chi}_1$) and the Goldstone mode ($\tilde{\chi}_2$). The inset in the figure shows the behaviour of $\tilde{\chi}_1$ and $\tilde{\chi}_2$ close to T_c .

fluctuations below T_c . Only the response of the system with respect to a modulated external field ($q_E = 2\pi/p$) can be infinite. The rapid decrease of χ_1 as $|\tau|$ increases depends on the fact that amplitude changes in the order parameters are energetically expensive except close to T_c^{20} .

The Goldstone mode contribution χ_2 , which is absent in the SmA phase, is the dominating part of χ in all the SmC* phase except close to T_c . It contributes with a broad maximum located at a temperature which is slightly less than the one where the maximum of the pitch is located. At T_c the Goldstone mode and the soft mode contribute equally to χ . This behaviour is a general feature of the model. The analytical expression of χ , which is given by Eqs. (II.57)–(II.59) and

(II.61) is unfortunately too involved to permit a perspicuous understanding of the behaviour of χ in terms of the parameters which enter the calculations. We can however make the following reasoning concerning the contribution to χ from the Goldstone mode. The coupling of \mathbf{P} to the external field increases with P_o . This suggests $\chi_2 \sim P_o^2$ as the response cannot depend on the sign of P_o . Further on, the elastic energy associated with the pitch is given by $g_{K_3} = (1/2)K_3q^2\theta_o^2$ (c.f. Eq. (II.3)). This suggests $\chi_2 \sim 1/K_3q^2\theta_o^2$. Altogether we thus expect the Goldstone mode part of the dielectric susceptibility to obey $\chi_2 \sim P_o^2p^2/K_3\theta_o^2$, a relation which is also dimensionally correct. In dimensionless form this relation reads $\tilde{\chi}_2 \sim (\tilde{P}_o\tilde{p}/\tilde{\theta}_o)^2$. If this relation is valid for all temperatures, it is also valid at T_c . As our model predicts $\tilde{\chi}_1(\tau = 0) = \tilde{\chi}_2(\tau = 0) = 1/2 \tilde{\chi}_A(\tau = 0)$, where $\tilde{\chi}_A$ is the dielectric susceptibility in the SmA phase, we get from Eq. (II.68)

$$\tilde{\chi}_2(\tau = 0) = \frac{1}{2} \frac{\beta^2 + \lambda^2}{(1 + \nu^2)(\beta^2 + \lambda^2) - (\beta - \lambda\nu)^2} \quad (\text{III.26})$$

From Eqs. (II.22) and (III.14) we further on get

$$\left(\frac{\tilde{P}_o\tilde{p}}{\tilde{\theta}_o} \right)^2 \Big|_{\tau=0} = 4\pi^2 \frac{\beta}{(\lambda + \nu\beta)^2} \quad (\text{III.27})$$

In the limit $\lambda, \nu, \delta < \beta$ the expressions on the right hand sides of Eqs. (III.26) and (III.27) are equal except concerning the numerical factors and we get

$$\frac{\tilde{\chi}_2}{\left(\frac{\tilde{P}_o\tilde{p}}{\tilde{\theta}_o} \right)^2} \Big|_{\tau=0} = \frac{1}{8\pi^2} \quad (\text{III.28})$$

We thus predict the following approximative relation to hold for the Goldstone mode of the dielectric susceptibility†

$$\tilde{\chi}_2 = \frac{1}{8\pi^2} \left(\frac{\tilde{P}_o\tilde{p}}{\tilde{\theta}_o} \right)^2 \quad (\text{III.29})$$

In order to verify the validity of Eq. (III.29) we calculated $\tilde{\chi}_2$ and $(\tilde{P}_o\tilde{p}/\tilde{\theta}_o)^2/8\pi^2$ for several sets of the parameters. In all cases the two

†This result can also be derived rigorously directly from Eqs. (II.56). See the footnote in the beginning of Section II.7.

curves agreed to such an extent that they were impossible to distinguish by the eye when plotted in the same figure. Rewriting Eq. (III.29) back to physical units we get

$$\chi_2 = \frac{1}{8\pi^2 K_3} \left(\frac{P_o p}{\theta_o} \right)^2 \tag{III.30}$$

We have tested the experimental validity of Eq. (III.30) by analysing our data of dielectric susceptibility,¹⁷ polarization⁶ and pitch^{10,11} for DOBAMBC, completed with the values of tilt given by Ostrovski et al.² In Table III we give the values of $(P_o p/\theta_o)^2/8\pi^2\chi_2$ in the temperature range where experimental data for all the involved quantities are available. We see that except close T_c , where the experimental uncertainty can be expected to be large, this ratio is constant to within five percent. In this way we thus have determined $K_3 \approx 3.8 \times 10^{-12}$ N, a value which should be compared to the value $K_3 = 3.4 \times 10^{-12}$ N which is given in Table II.

In conclusion we summarize that our model is capable of describing the temperature dependence of the dielectric susceptibility of the ferroelectric SmC* phase in good agreement with experiments. The analytical expression of χ is however much too involved to permit any statements of the influence of the different parameters on the

TABLE III

Experimental test of the proposed behaviour of the Goldstone mode contribution to the dielectric susceptibility. If Eq. (III.30) is valid, the numbers which are given in the right column shall be constant and equal to the elastic constant K_3 . We see that except close to T_c , the numbers given in the right column are constant within five per cent. Thus the table supports the validity of Eq. (III.30).

$T_c - T [K]$	$\chi_2 \times 10^{11} [C/Vm]$	$\frac{1}{8\pi^2} \left(\frac{P_o p}{\theta_o} \right)^2 \times 10^{22} [CN/Vm]$	$\frac{1}{8\pi^2 \chi_2} \left(\frac{P_o p}{\theta_o} \right)^2 \times 10^{12} [N]$
1.2	1.5	0.4	2.6
1.6	2.2	0.8	3.6
2.3	3.4	1.4	4.0
2.7	4.2	1.6	3.9
3.3	4.9	1.8	3.7
3.8	5.2	1.9	3.7
4.3	5.1	1.9	3.8
4.8	4.9	1.9	3.9
5.6	4.6	1.9	4.0
6.1	4.5	1.8	4.0
6.7	4.3	1.7	4.0

shape of χ . Concerning the Goldstone mode, which is the dominant part of χ , we have however derived the approximate expressions (III.29) and (III.30). By these we can indirectly, from the discussion of the temperature dependence of polarization/tilt and pitch in Section III.4 and III.5, relate χ_2 to the parameters of the model. It is also clear from numerical calculations that the “small” parameters λ , ν and δ are essential tools in order to describe χ_2 correctly. Early attempts^{16,33} of calculating χ_2 , using a simplified free-energy density where the d -term as well as η -term and the Ω -term are missing, have failed and predict just $\chi_2 = \text{constant}$. This result is obvious in the light of Eq. (III.29) as this simplified free-energy density predicts²³ both \bar{q} and $\bar{P}_o/\bar{\theta}_o$ to be constant. This again emphasizes the importance of the Ω -term, which is responsible for the S-shape of the $\bar{P}_o/\bar{\theta}_o$ curve and of the d -term, which is responsible for the monotonous increase of pitch with temperature at low temperatures.

III.7 The heat capacity

The heat capacity of the system is calculated simply by the use of Eq. (II.73). In order to describe heat capacity data in a proper way the sixth-order term in tilt (the c -term) was added^{19,20} to the free-energy density of the system. In the simple model, used by the authors of references 19 and 20, only the α -, b - and c -term in the free-energy density of Eq. (II.1) were retained. It is then easily proven that in the case $c = 0$ the heat capacity gets a triangular shape while the introduction of the c -term gives the heat capacity a more realistic bent shape.

In our dimensionless model the c -term is substituted by the ρ -term as is seen from the definition of Eqs. (II.13) and (II.15). Also here we have found that the ρ -term is essential in describing the heat capacity correctly. In Figure 15 we show a sequence of calculated \bar{C}_p curves using different values of ρ while the other parameters are taken to be $\gamma = 2.0$; $\beta = 0.2$; $\lambda = 0.06$; $\nu = -0.06$ and $\delta = 0.02$. We note that for $\rho = 0$ the heat capacity develops a maximum which is located approximately 1K below T_c . Increasing ρ , this maximum disappears and more realistic \bar{C}_p curves are produced. When ρ and γ are comparable in magnitude, \bar{C}_p adopts a form which is in qualitative agreement with experiments. Increasing ρ further \bar{C}_p gets too steep. This sequence of curves clearly demonstrates the influence of the ρ -term when calculating the heat capacity of the system. We thus conclude that we shall choose a value of ρ which is comparable in magnitude to γ in order to get a realistic shape of the calculated heat capacity of the system.

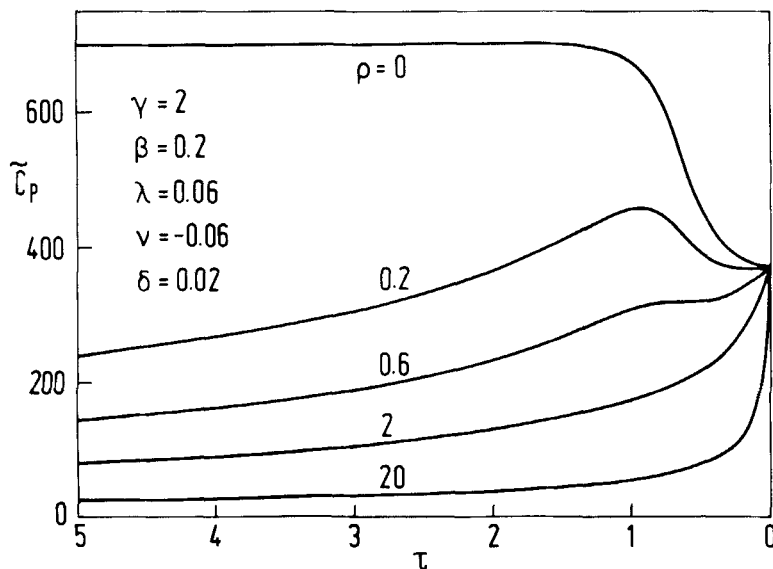


FIGURE 15 Influence of the parameter ρ on the temperature dependence of the heat capacity.

IV DISCUSSION

This paper presents a unified thermodynamic model of the ferroelectric SmC^* phase. The basis of the model is the Landau expansion of the free-energy density given by Eq. (II.1). By this expansion eleven material parameters are introduced into the problem. In order to get any useful information out of the model there are two things which we must master. First of all we must understand how the parameters entering Eq. (II.1) determine the behaviour of the solutions of the governing equations and secondly we must be able to establish these parameters from experimental data in a unique (and straightforward) way.

Compared with previous models,^{22,23} the predictions of which imply the three quantities pitch, the ratio polarization/tilt and the Goldstone mode contribution to the dielectric susceptibility to be temperature independent, our model includes another three terms in the Landau expansion of the free-energy density. These are the terms connected to the constants d , η and Ω in Eq. (II.1). The introduction of the d term is equivalent to replacing Λ by $\Lambda + d\theta^2$ and is made in order to describe the monotonous increase of the pitch with temperature

far from T_c . The Ω term, which leads to a transverse quadrupole ordering, is of non-chiral character and is therefore expected to be large compared to the bilinear coupling (the C term), which is of chiral character. Thus a cross-over behaviour can be expected from the regime close to T_c , where because of small θ only bilinear coupling is important, to the regime far from T_c , where θ is large and the biquadratic coupling induces a transverse quadrupole ordering. This cross-over is clearly demonstrated to occur for small values of the parameter z in Figures 7–9 and 11. From the definition of β ($\beta = \eta^{1/2} \tilde{C} / \Omega^{1/2}$) it is clear that the larger the influence of the biquadratic coupling ($\sim \Omega$) is compared to the bilinear coupling ($\sim \tilde{C}$), the smaller is β and thus the importance of the biquadratic coupling is established.

In order to simplify the model we introduced the dimensionless form of writing the equations in Section II.4. By doing so we transformed the original set of eleven parameters into a set of eleven new ones. The advantage of doing so is that in the dimensionless form of the model the parameters enter the calculations in different levels. Only six of the constants are needed in order to calculate the temperature dependence of physical quantities of the system. These are the six dimensionless parameters which are defined by Eqs. (II.13) and (II.15). Concerning these parameters we have shown by available experimental data and by some fundamental theoretical considerations that we can establish the following general feature of the parameters: $\gamma > 1$; $\rho \sim \gamma$; $|\beta| < 1$; $|\lambda|$, $|\nu|$, $|\delta| < |\beta|$. While γ and ρ are always positive, the signs of the parameters β , λ , ν and δ have to be chosen according to the discussion of Section II.5.

In Section III.4 we showed that by making a decent approximation only the parameter β enters the calculations of the polarization/tilt ratio as a function of tilt-squared. We also showed that essentially only the parameter β determines the qualitative behaviour of as well tilt as polarization versus temperature. The parameters γ and ρ mainly introduce saturation effects far from T_c . In the general discussion of the shape of tilt and polarization we thus can limit ourselves to use the three parameters γ , β and ρ . The importance of ρ when discussing the heat capacity of the system is demonstrated in Figure 15.

Discussing the pitch and the dielectric susceptibility of the system also the parameters λ , ν and δ have to be considered. The expression of the wave-vector of the pitch given by Eq. (II.22) is straightforward and permits us to describe its temperature dependence in terms of the “small parameters” λ , ν and δ and of the ratio $\tilde{P}_o/\tilde{\theta}_o$ (c.f. Figure 12), which in turn is determined mainly by the parameter β . Concerning the dielectric susceptibility, the general expression of which

is given by Eqs. (II.57)–(II.59) and (II.61) only numerical calculations are permitted due to the complicated structure of these expressions. However, the approximation of the contribution to χ from the Goldstone mode (Eq. (III.29)) which we derived by physical reasoning connects the understanding of its behaviour to the understanding of the behaviour of $\tilde{P}_o/\tilde{\theta}_o$ and \tilde{p} . As \tilde{p} is a function of $\tilde{P}_o/\tilde{\theta}_o$ we notice that also χ_2 can be discussed in terms of $\tilde{P}_o/\tilde{\theta}_o$. This again demonstrates the importance of the parameter β .

Finally the scaling factors enter the calculations. As we have scaled as well temperature as the physical quantities this incorporation is not straightforward. Once we however can determine one of the scaling factors, the rest can simply be determined by comparing the outcome of the calculations with experimental data.

In order to determine the complete set of parameters for a certain compound we can proceed in two alternative ways. The parameters of DOBAMBC which are given in Table II were determined by fitting the outcome of the calculations with available experimental data. The fitting is of course a very hard problem to approach as we are working effectively in an eleven-dimensional parameter space. Thus other methods of analysing the experimental data should be found. One way is to determine the parameters one or two at a time by comparing certain features of the experimental curves with the predictions of the governing equations. Carefully obtained experimental data of tilt and polarization enable use for instance to determine β by investigating the shape of the P_o/θ_o versus θ_o^2 curve. Knowing β the ratio of the scaling factors P_o^*/θ_o^* can be determined as we know from Eq. (III.14) that $\lim_{\tau \rightarrow 0} \tilde{P}_o/\tilde{\theta}_o = \beta$. In this way we believe that by a thorough analytical investigation of the governing equations, accompanied with a carefully determined set of experimental data, it should be possible to determine all the parameters of the model unambiguously.

In some recent papers^{7,30,34} Huang and coworkers present measurements of the tilt, polarization and heat capacity of DOBAMBC. To analyse their data they employ a Landau expansion which is identical to the one we are using in this paper. Concerning the experimental data the values of Huang et al. agree with ours except at one point. While we are observing an S-shaped behaviour of the polarization curve, Huang et al. do not. We have argued in Section III.4 (see also Refs. 35 and 36) that one should expect to observe a cross-over behaviour of the polarization curve due to the competition between the bilinear (the C-term) and the biquadratic (the Ω -term) coupling terms in the free-energy density expansion. This kind of

cross-over behaviour is also observed experimentally in other compounds.^{8,9} Concerning the fitting of the theory to the experimental data Huang et al. seem to experience the same problems as we do. When including the pitch measurements of Refs. 11 or 15 into their data, they are only able to produce fittings that are qualitatively, but not quantitatively, correct. This emphasizes the statement above that more work has to be done concerning the determination of the material parameters of the model. In Table II we compare the values of these parameters as they are obtained by us and by Huang et al.³⁰ We notice that for most parameters the agreement is good. The difference in some signs is due to the fact that while we are describing a LH(−) compound, Huang et al. are describing a RH(+) compound (The notation of LH(−) and RH(+) compounds is introduced in Section II.5 (c.f. Figure 2)).

Because of the emerging practical applications of SmC* liquid crystal to electro-optic devices the access to a realistic model of the system along with a straightforward way of determining the corresponding material constants is of importance. We believe that our model after a deeper investigation of the determination of the material parameters can provide such a model. Once this is established, the important investigations of connecting the parameters to molecular structure and to derive expression which rules the behaviour of the parameters by the mixing of different compounds can get started. Thus our model should be able to provide good tools for everybody who is interested in investigating or predicting the behaviour of the ferroelectric SmC* phase.

References

1. R. B. Meyer, L. Leibert, L. Strzelecki and P. Keller, *J. Physique Lett.*, **36**, L69 (1975).
2. B. I. Ostrovski, A. Z. Rabinovich, A. S. Sonin, B. A. Strukov and S. A. Taraskin, *Ferroelectrics*, **20**, 189 (1978).
3. P. Martinot-Lagarde, R. Duke and G. Durand, *Mol. Cryst. Liq. Cryst.*, **75**, 249 (1981).
4. J. Hoffman, W. Kuczynski and J. Malecki, *Mol. Cryst. Liq. Cryst.*, **44**, 287 (1978).
5. K. Skarp, I. Dahl, S. T. Lagerwall and B. Stebler, *Mol. Cryst. Liq. Cryst.*, **114**, 283 (1984).
6. C. Filipič, A. Levstik, I. Levstik, R. Blinc, B. Žekš, M. Glogarova and T. Carlsson, *Ferroelectrics*, **73**, 295 (1987).
7. S. Dumrongrattana and C. C. Huang, *Phys. Rev. Lett.*, **56**, 464 (1986).
8. G. Andersson, personal communications.
9. D. S. Parmar, M. A. Handschy and N. A. Clark, poster presented at the 11th International Liquid Crystal Conference, Berkeley, 1986.

10. R. Blinc, B. Žekš, I. Muševič and A. Levstik, *Mol. Cryst. Liq. Cryst.*, **114**, 189 (1984).
11. I. Muševič, B. Žekš, R. Blinc, L. Jansen, A. Seppen and P. Wyder, *Ferroelectrics*, **58**, 71 (1984).
12. K. Yoshino, T. Uemoto and Y. Inuishi, *Jap. J. Appl. Phys.*, **16**, 571 (1977).
13. A. Levstik, B. Žekš, I. Levstik, R. Blinc and C. Filipič, *J. Physique C3*, **40**, C3-303 (1979).
14. M. Glogarova and J. Pavel, *Mol. Cryst. Liq. Cryst.*, **114**, 249 (1984).
15. B. I. Ostrovski, A. Z. Rabinovich, A. S. Sonin and B. A. Strukov, *Zh. Eksp. Teor. Fiz.*, **74**, 1748 (1978).
16. L. G. Benguigui, *Ferroelectrics*, **58**, 269 (1984).
17. A. Levstik, T. Carlsson, C. Filipič and B. Žekš, *Mol. Cryst. Liq. Cryst.*, **154**, 259 (1988).
18. A. Levstik, T. Carlsson, C. Filipič, I. Levstik and B. Žekš, *Phys. Rev. A*, **35**, 3527 (1987).
19. C. C. Huang and J. M. Viner, *Phys. Rev.*, **A25**, 3385 (1982).
20. T. Carlsson and I. Dahl, *Mol. Cryst. Liq. Cryst.*, **95**, 373 (1983).
21. S. C. Lien, C. C. Huang, T. Carlsson, I. Dahl and S. T. Lagerwall, *Mol. Cryst. Liq. Cryst.*, **108**, 149 (1984).
22. S. A. Pikin and V. L. Indenbom, *Uspekhi Fiz. Nauk*, **125**, 251 (1978).
23. R. Blinc and B. Žekš, *Phys. Rev.*, **A18**, 740 (1978).
24. B. Žekš, *Mol. Cryst. Liq. Cryst.*, **114**, 259 (1984).
25. N. A. Clark and S. T. Lagerwall, *Ferroelectrics*, **59**, 25 (1984).
26. R. Blinc, C. Filipič, A. Levstik, B. Žekš and T. Carlsson, Proceedings of the Fifth European Winter Liquid Crystal Conference, Borovec, Bulgaria, March 25–30, 1987, *Mol. Cryst. Liq. Cryst.*, **151**, 1 (1987).
27. R. Blinc, M. Luzar, J. Seliger and V. Rutar, in "Liquid Crystals of One and Two-Dimensional Order," W. Helfrich, G. Heppke, Editors, Springer-Verlag, Berlin (1980), p. 34.
28. M. Luzar, V. Rutar, J. Seliger and R. Blinc, *Ferroelectrics*, **58**, 115 (1984).
29. R. Blinc, M. Vilfan, and J. Seliger, *Bull. Mag. Res.*, **5**, 51 (1983).
30. C. C. Huang and S. Dumrongrattana, *Phys. Rev. A*, **34**, 5020 (1986).
31. T. Carlsson, B. Žekš, A. Levstik, C. Filipič, I. Levstik and R. Blinc, *Phys. Rev. A*, **36**, 1484 (1987).
32. J. W. Goodby, E. Chin, J. M. Geary and J. S. Patel, poster presented at the 11th International Liquid Crystal Conference, Berkeley, 1986.
33. P. Martinot-Lagarde and G. Durand, *J. Physique Lett.*, **41**, L43 (1980).
34. S. Dumrongrattana, C. C. Huang, G. Nounesis, S. C. Lien and J. M. Viner, *Phys. Rev. A*, **34**, 5010 (1986).
35. B. Žekš, T. Carlsson, C. Filipič and A. Levstik, Proceedings of the Fifth European Winter Liquid Crystal Conference, Borovec, Bulgaria, March 25–30, 1987, *Mol. Cryst. Liq. Cryst.*, **151**, 109 (1987).
36. B. Žekš, T. Carlsson, C. Filipič and A. Levstik, *Phys. Rev. Lett.*, **59**, 1869 (1987).